Supplementary Information

Discovery of Antibacterial Manganese(I) Tricarbonyl Complexes through Combinatorial Chemistry

Mirco Scaccaglia[1,3], Michael P. Birbaumer[3], Silvana Pinelli[2], Giorgio Pelosi[1], Angelo Frei[3]

[1] Department of Chemistry, Life Sciences and Environmental Sustainability, University of Parma, 43124 Parma, Italy
[2] Department of Medicine and Surgery, University of Parma, Via Gramsci 14, 43126 Parma, Italy;
[3] Department of Chemistry, Biochemistry & Pharmaceutical Sciences, University of Bern, Freiestrasse 3, 3012 Bern, Switzerland

Part 1: Supplementary Figures and Tables

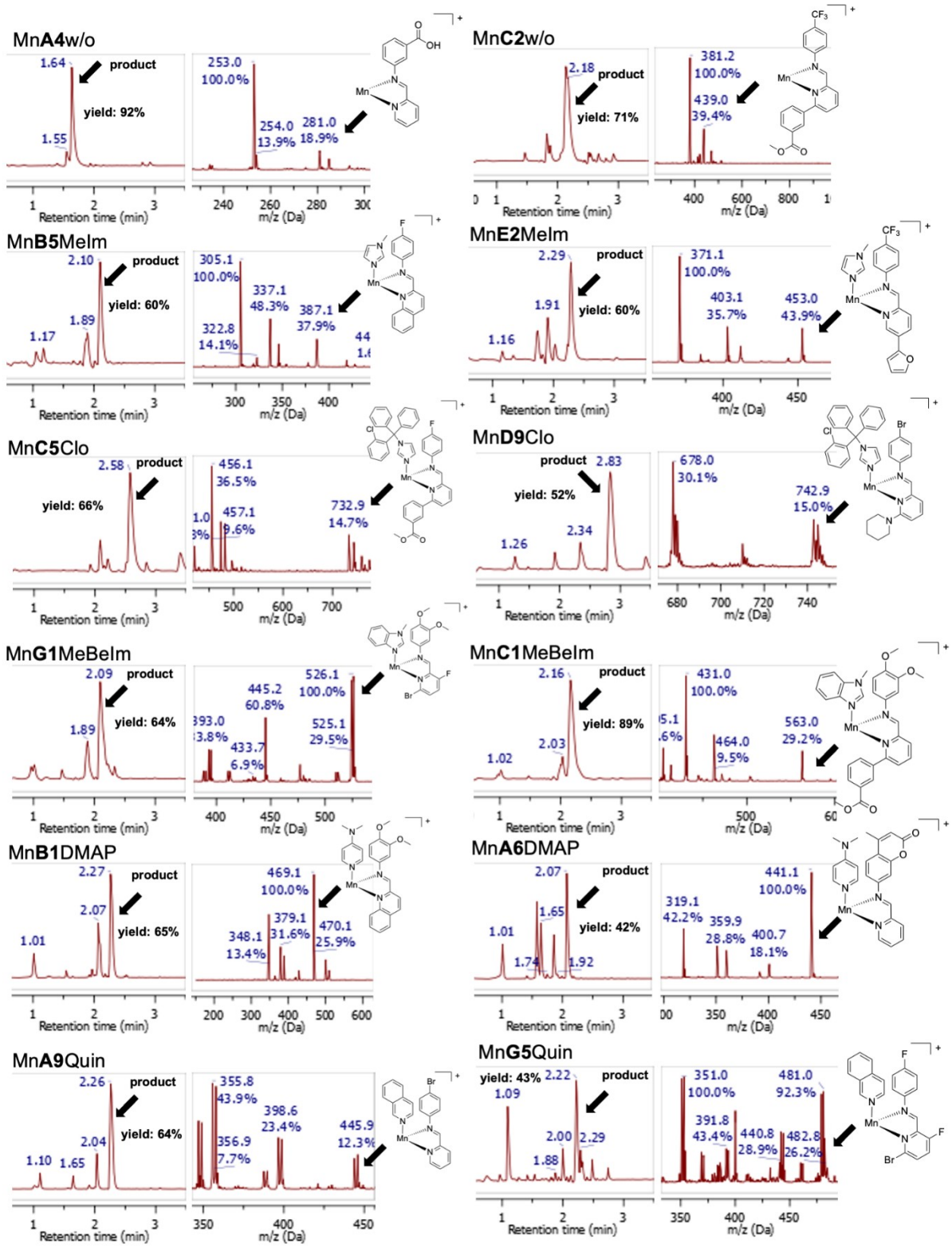

Figure S1. Representative chromatogram depicting the product peak and yield, along with their corresponding MS spectra indicating the molecular fragments within a selected sample from the crude reaction mixture during combinatorial synthesis.

Solvent

	1	2	3	4	5	6	7	8	9	10
A		50							50	>100
B		>100				>100		>100	>100	
C	50	50			100-50	>100	50	25	50-25	
D	50	50			100	>100	50	50-25	50-25	
E	>100	50	>100		100	>100	100	50	>100	50
F										
G										

MeIm

	1	2	3	4	5	6	7	8	9	10
A								100-50	100-50	
B	>100							>100	>100	
C	25	50-100	>100		25	>100	50	25	>100	
D	100	>100			100		50	50	>100	
E	>100	100			>100	>100	>100	100	>100	
F										
G		>100			50-100		50	>100	>100	

Clo

	1	2	3	4	5	6	7	8	9	10
A			3.12	25.00			3.12			
B							3.12			
C										
D										
E										
F										
G										

MeBeIm

	1	2	3	4	5	6	7	8	9	10
A		25			100-50	100	100	25	12.5	
B	>100	100			100-50	>100	50	25-12,5	25	
C	12.5	12.5			12,5-6,25	50	6.25	3.12	6.25	100
D	50	25-12,5			50-25	100	50	25	12.5	100
E	50	12.5	100		25	25	25			
F	50							>100		
G	50	>100			12.5		12.5	12.5	6.25	

DMAP

	1	2	3	4	5	6	7	8	9	10
A		12.50			25.00		12.50	6.25	6.25	
B	3.13	25-12,5			6.25	50.00	6.25	3.13	3.13	
C	1.56	6.25			3.13	12.50	3.13	1.56	3.13	25.00
D	6.25	6.25			6.25	12.50	3.13	1.56	3.13	12.50
E	6.25	6.25			3.13	12.50	50.00	1.56	3,13 - 1,56	100-25
F	50-12,5							50.00		
G							50.00	12.50	50.00	

Quin

	1	2	3	4	5	6	7	8	9	10
A								25	12.5	
B	50	100			25		25	6.25	25	
C	12.5	12.5			12.5	25	12.5	3.13	3.13	
D	50	25			50	50	50	12.5	12.5	
E	25	6.25			12.5	6.26	25	6.25	6.25	100-25
F										
G	25				25		12.5	3.13		

Table S1. Overview of antibacterial activity display as MIC [µM] of the 420 combinatorial manganese complexes against MRSA.

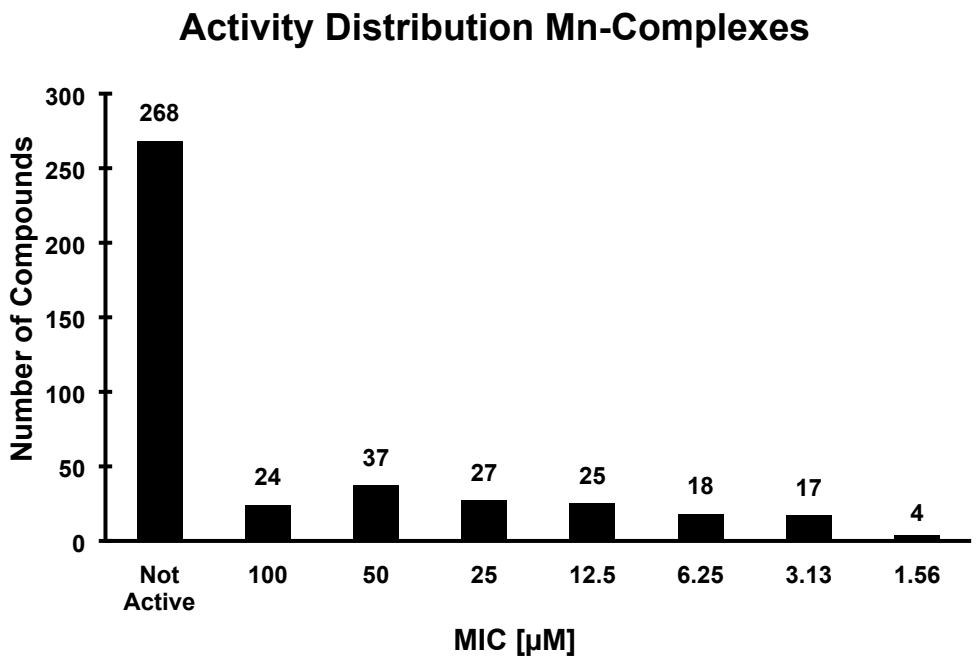

Figure S2. Distribution of the manganese compounds based on their activity against MRSA, represented as MIC [µM].

Amines			Aldehydes			Axial Ligands		
	MRSA	E. coli		MRSA	E. coli		MRSA	E. coli
1	> 100	> 100	**A**	> 100	> 100	**MeIm**	> 100	> 100
2	> 100	> 100	**B**	> 100	> 100	**Clo**	12.5	> 100
3	> 100	> 100	**C**	> 100	> 100	**BeMeIm**	> 100	> 100
4	> 100	> 100	**D**	> 100	> 100	**DMAP**	> 100	> 100
5	> 100	> 100	**E**	> 100	> 100	**Quin**	> 100	> 100
6	> 100	> 100	**F**	> 100	> 100			
7	> 100	> 100	**G**	> 100	> 100			
8	> 100	> 100						
9	> 100	> 100						
10	> 100	> 100						

Table S2. Antibacterial activity display as MIC [µM] of the building blocks combinatorial against MRSA and E. coli.

	MnD8DMAP	MnC1DMAP	MnG9MeBeIm
Mn – N_{ax}	2.094(2)	2.082(2)	2.086(3)
Mn – N_{py}	2.103(2)	2.123(3)	2.132(3)
Mn – N_{am}	2.050(2)	2.050(3)	2.056(3)
Mn – $CO_{(trans\ ax)}$	1.806(2)	1.813(3)	1.829(4)
Mn – $CO_{(trans\ py)}$	1.798(2)	1.806(4)	1.799(4)
Mn – $CO_{(trans\ am)}$	1.827(2)	1.820(4)	1.826(5)

Table S3. Selected Bond Lengths (Å) Legend: ax (axial), py (pyridine ring), am (amine).

	MIC [μM] vs. Gram-negative Bacteria			
	A. baumannii	***P. aeruginosa***	***K. pneumonia***	**E. coli**
MnC5MeIm	> 100	>100	>100	> 100
MnA3Clo	50	>100	>100	> 100
MnC8MeBeim	100-50	>100	>100	> 100
MnC9MeBeim	25	>100	>100	> 100
MnE2MeBeim	25	>100	>100	> 100
MnG9MeBeim	100	>100	>100	100-50
MnC1DMAP	100	>100	>100	> 100
MnD8DMAP	25	>100	>100	100-50
MnD9DMAP	>100-50	>100	>100	50-25
MnE6Quin	>100	>100	>100	> 100
PMX [μg/mL]	0.25	1	2	1

Table S4. Antibacterial activity is displayed as MIC [μM]. PMX – Polymixin B

	MBC [μM] vs. MRSA
MnC5MeIm	50-25
MnA3Clo	3.13
MnC8MeBeim	6.25
MnC9MeBeim	6.25
MnE2MeBeim	6.25
MnG9MeBeim	1.56
MnC1DMAP	6.25-3.13
MnD8DMAP	6.25-3.13
MnD9DMAP	6.25-3.13
MnE6Quin	12.5-6.25
VAN [ug/mL]	8

Table S5. Antibacterial activity is displayed as MBC [μM]. VAN – Vancomycin

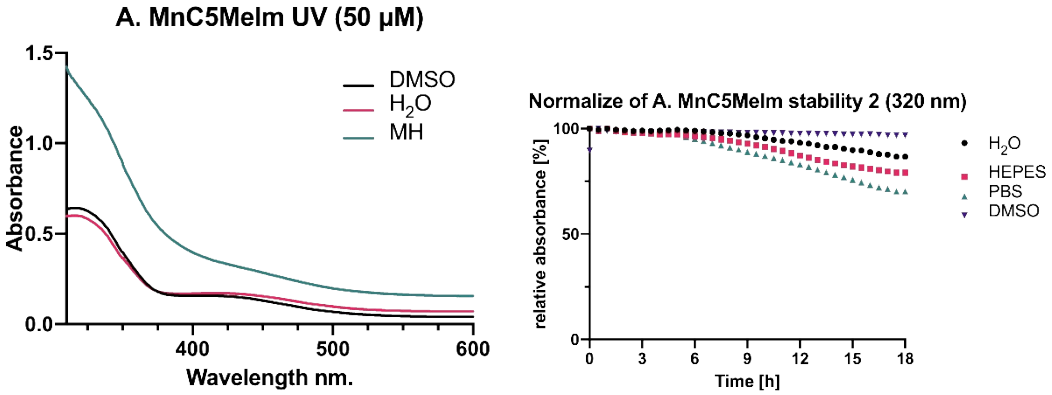

Figure S3. UV-Vis spectra of **MnC5MeIm** (left) and stability over 18 hours, monitored at the maximum absorbance (right).

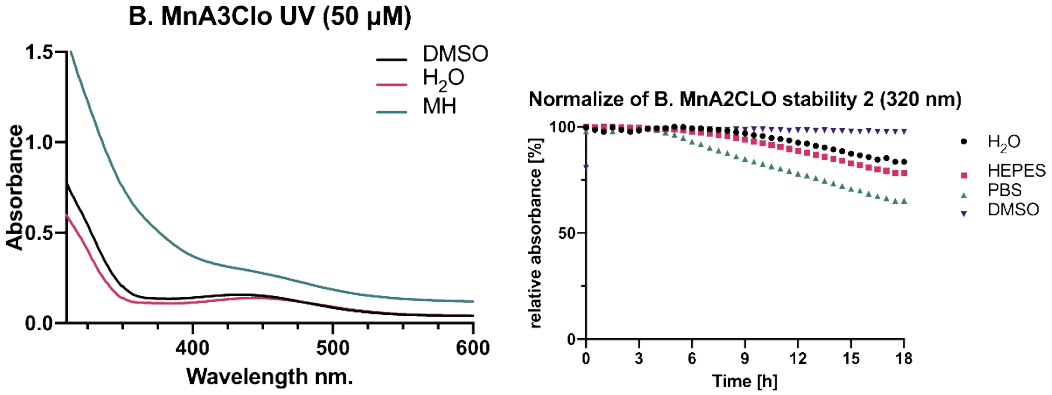

Figure S4. UV-Vis spectra of **MnA3Clo** (left) and stability over 18 hours, monitored at the maximum absorbance (right).

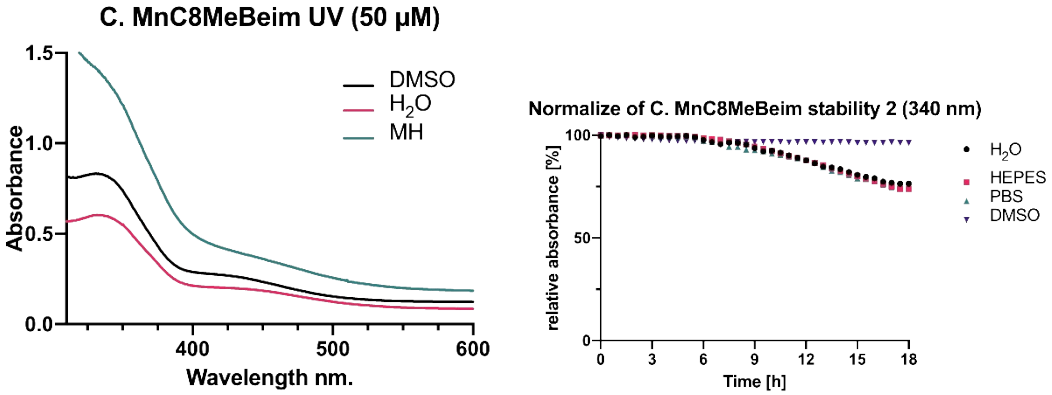

Figure S5. UV-Vis spectra of **MnC8MeBeim** (left) and stability over 18 hours, monitored at the maximum absorbance (right).

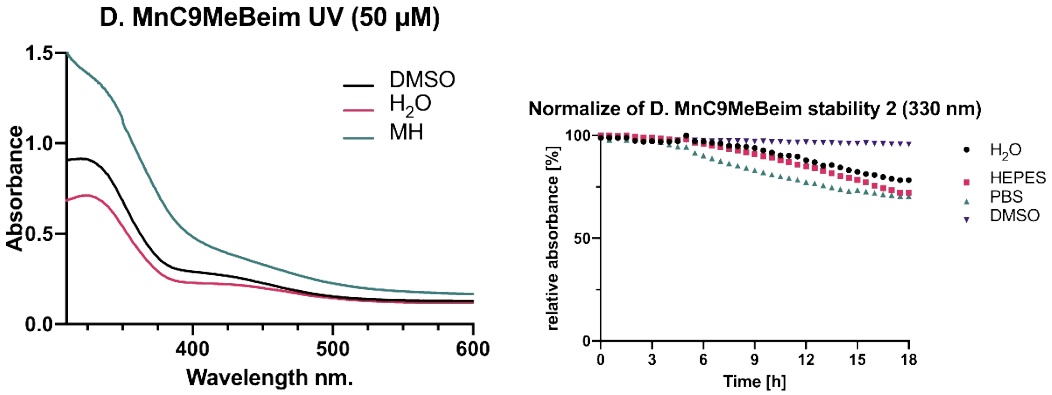

Figure S6. UV-Vis spectra of **MnC9MeBeIm** (left) and stability over 18 hours, monitored at the maximum absorbance (right).

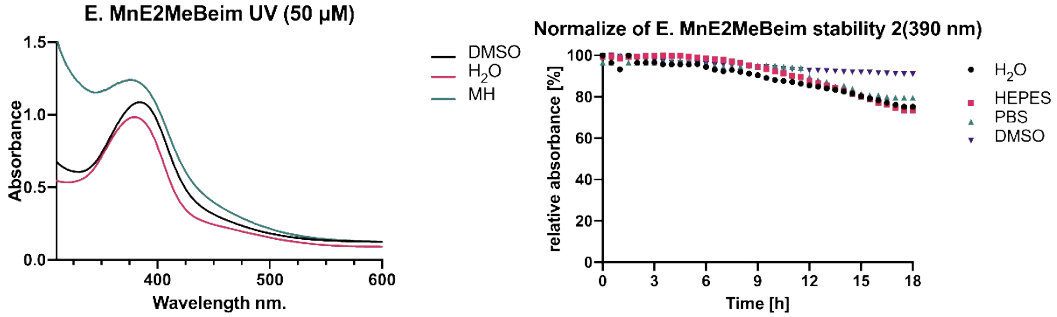

Figure S7. UV-Vis spectra of **MnE2MeBeIm** (left) and stability over 18 hours, monitored at the maximum absorbance (right).

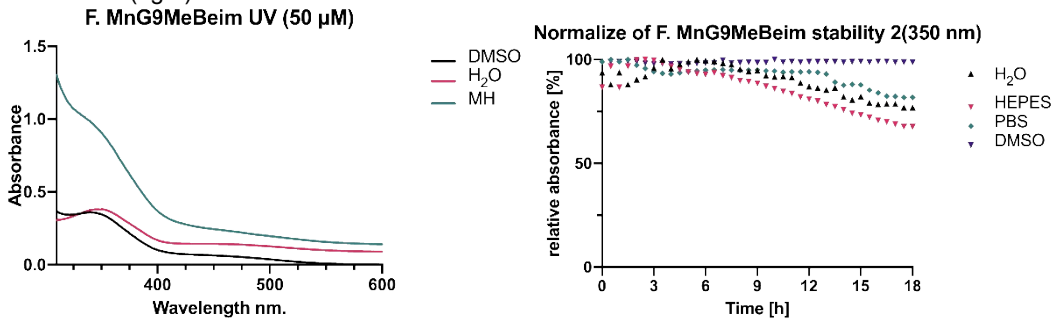

Figure S8. UV-Vis spectra of **MnG9MeBeIm** (left) and stability over 18 hours, monitored at the maximum absorbance (right).

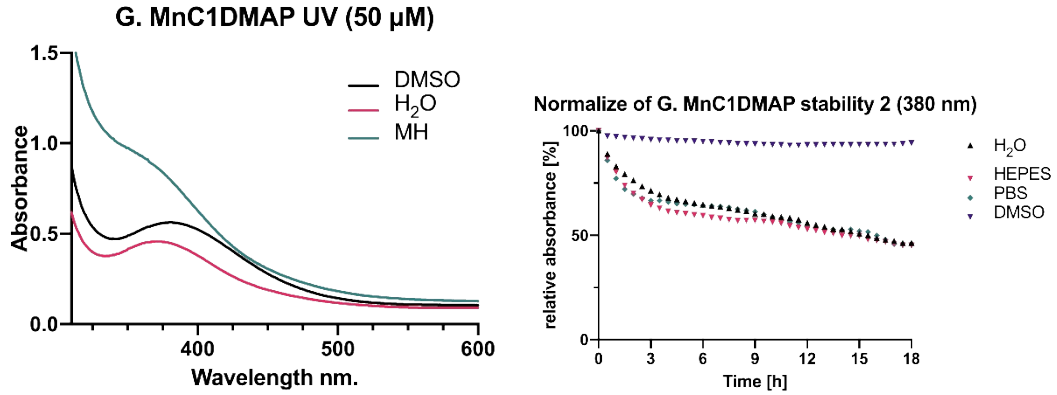

Figure S9. UV-Vis spectra of **MnC1DMAP** (left) and stability over 18 hours, monitored at the maximum absorbance (right).

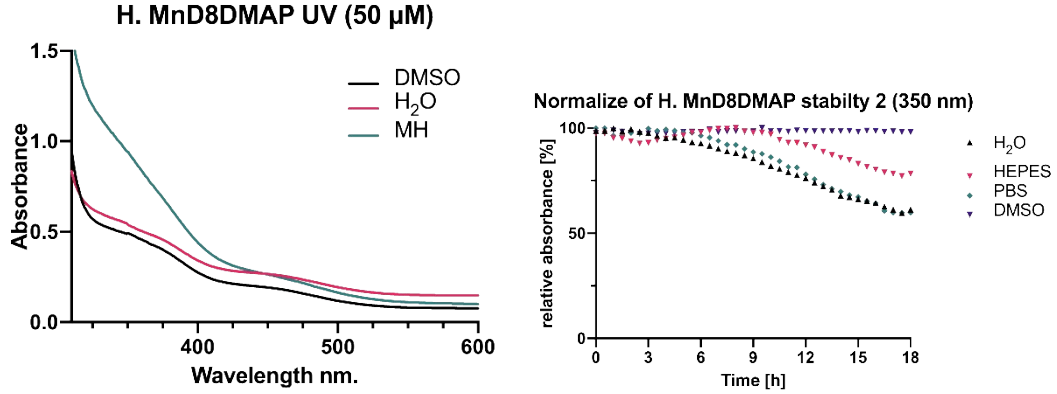

Figure S10. UV-Vis spectra of **MnD8DMAP** (left) and stability over 18 hours, monitored at the maximum absorbance (right).

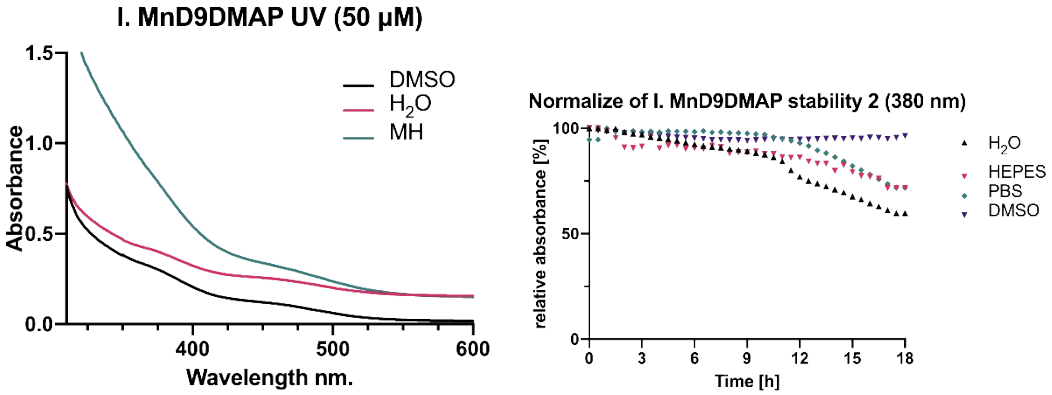

Figure S11. UV-Vis spectra of **MnD9DMAP** (left) and stability over 18 hours, monitored at the maximum absorbance (right).

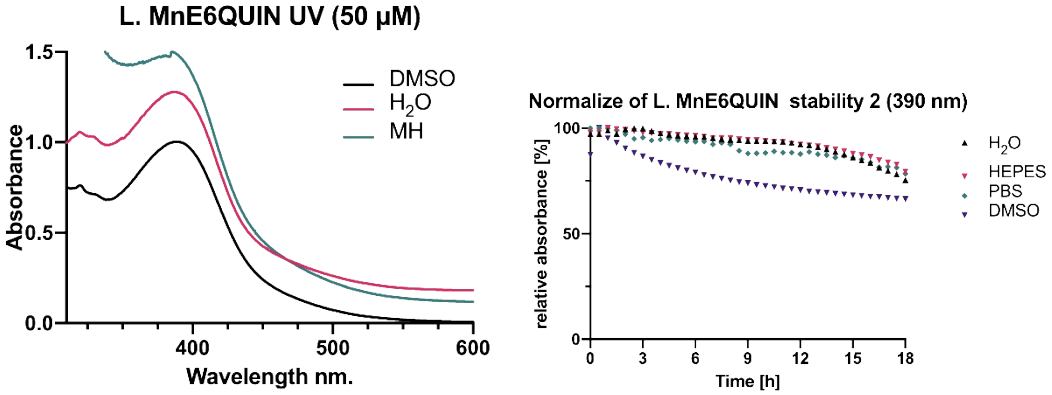

Figure S12. UV-Vis spectra of **MnE6Quin** (left) and stability over 18 hours, monitored at the maximum absorbance (right).

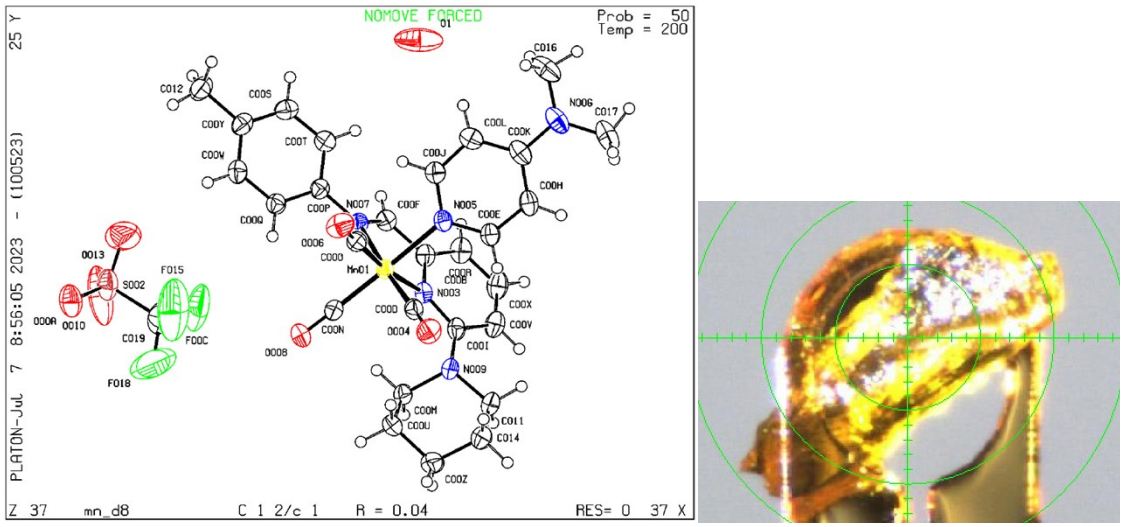

Figure S13. Crystal structure of **MnD8DMAP** (CCDC No. 2280008). The right panel shows the crystal structure with atom labeling. The left panel shows the crystal used to collect the structure.

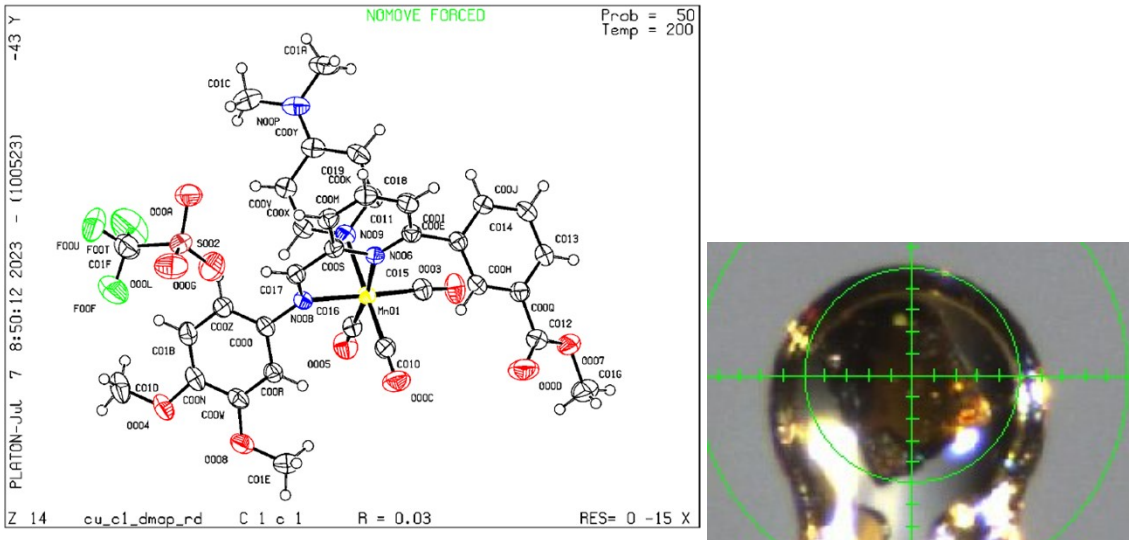

Figure S14. Crystal structure of **MnC1DMAP** (CCDC No. 2280009). The right panel shows the crystal structure with atom labeling. The left panel shows the crystal used to collect the structure.

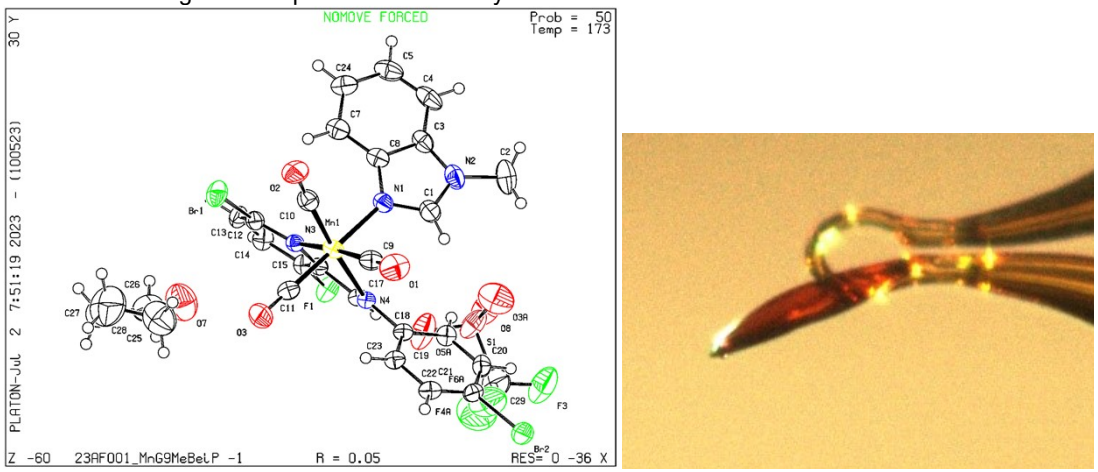

Figure S15. Crystal structure of **MnG9MeBeim** (CCDC No. 2280010). The right panel shows the crystal structure with atom labeling. The left panel shows the crystal used to collect the structure.

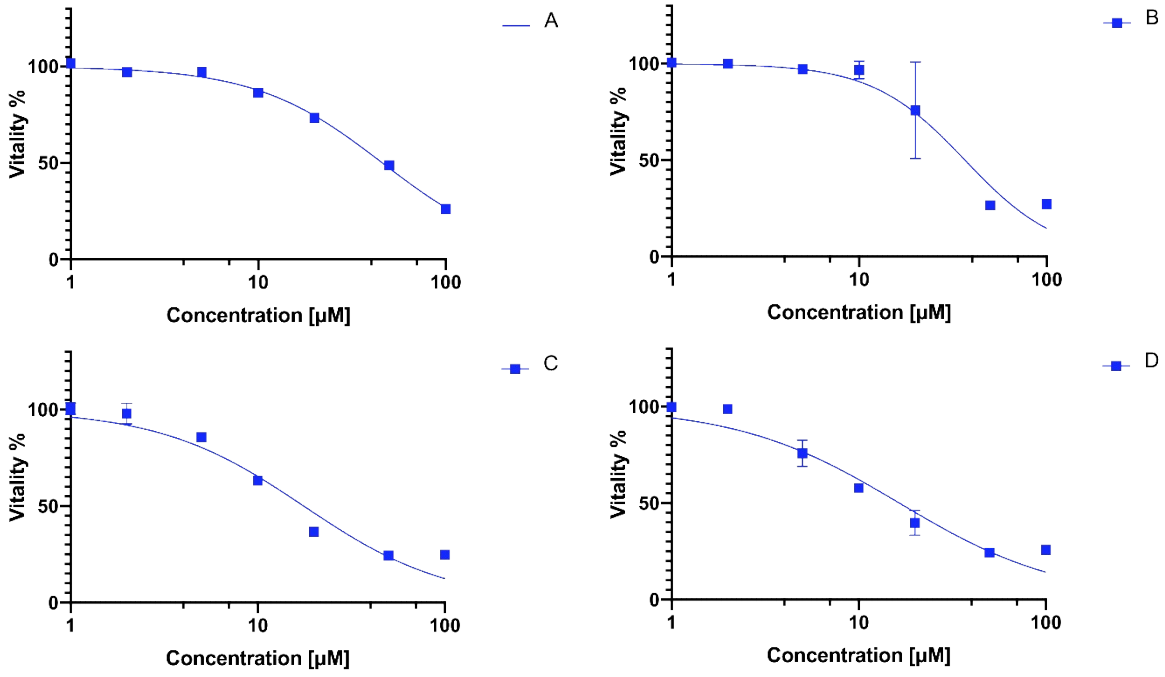

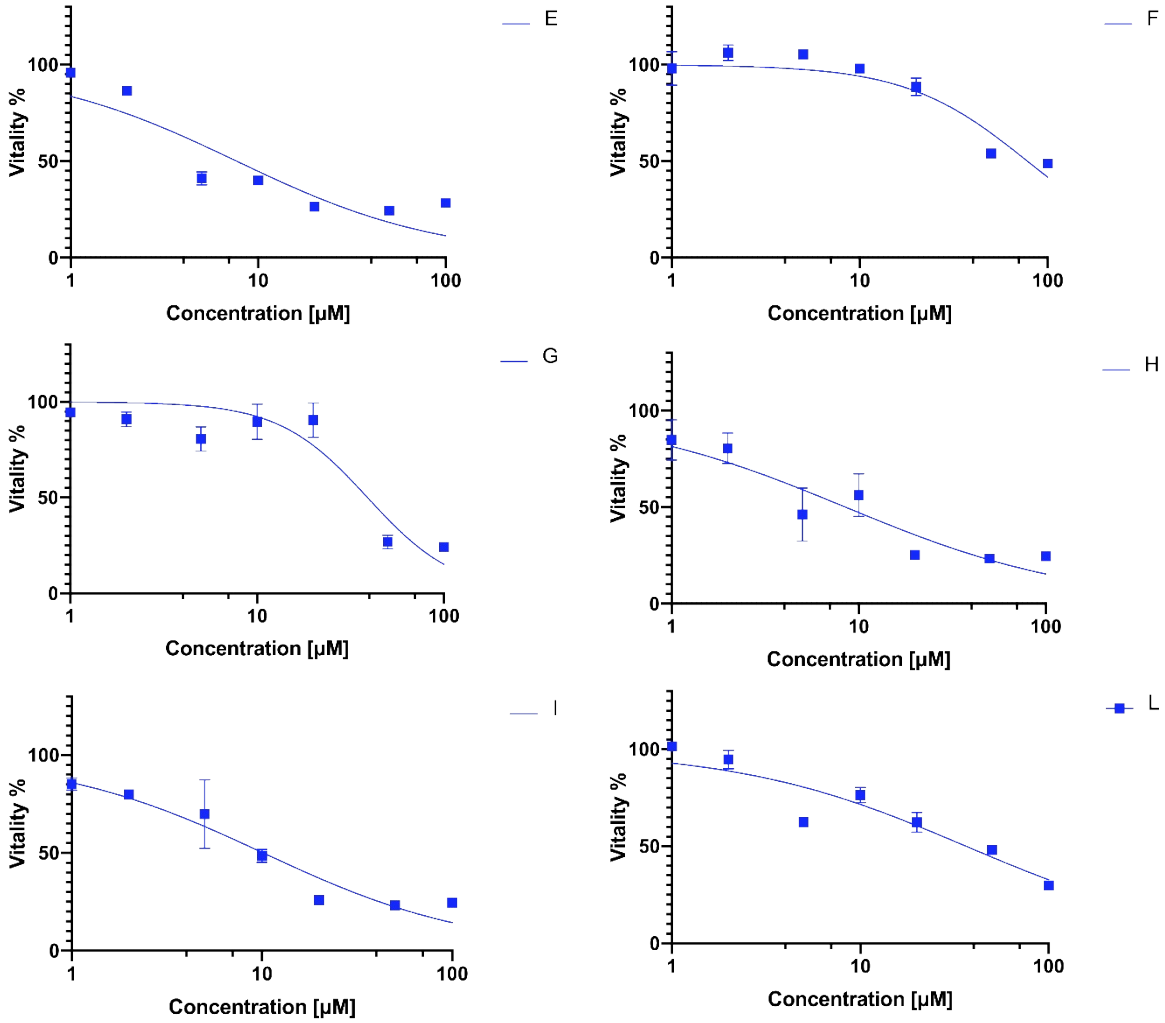

Figure S16. Vitality of the HuDe cells against different concentration of Mn complex (A – MnC5MeIm, B – MnA3Clo, C – MnC8MeBeIm, D – MnC9MeBeIm, E – MnE2MeBeIm, F – MnG9MeBeIm, G – MnC1DMAP, H – MnD8DMAP, H – MnD9DMAP, I – MnE6Quin). Interpolation curve to evaluate the CC_{50} is also displayed.

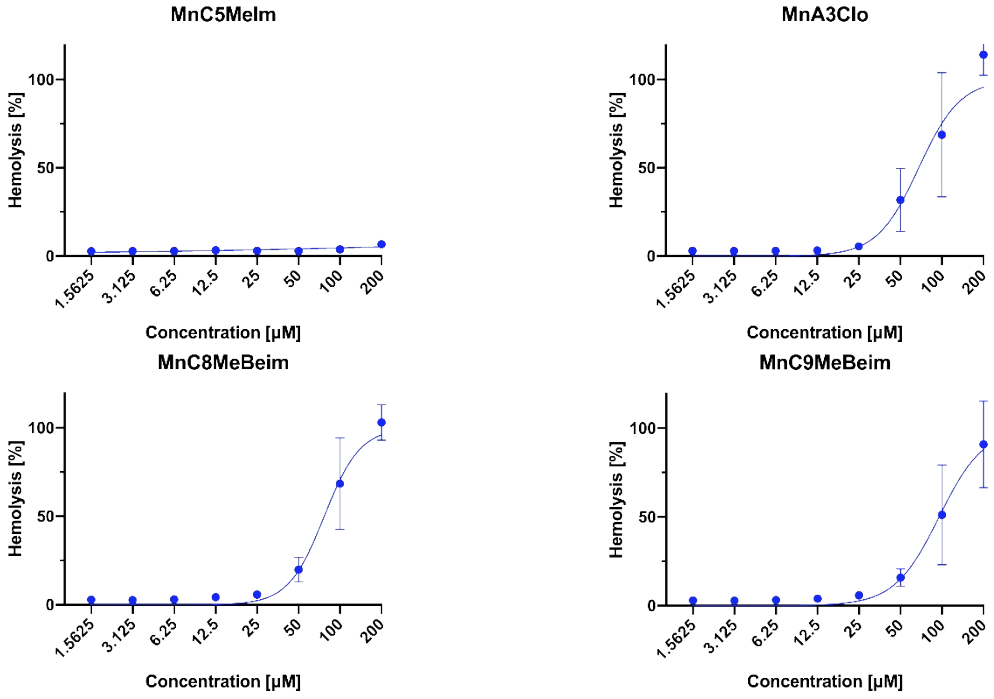

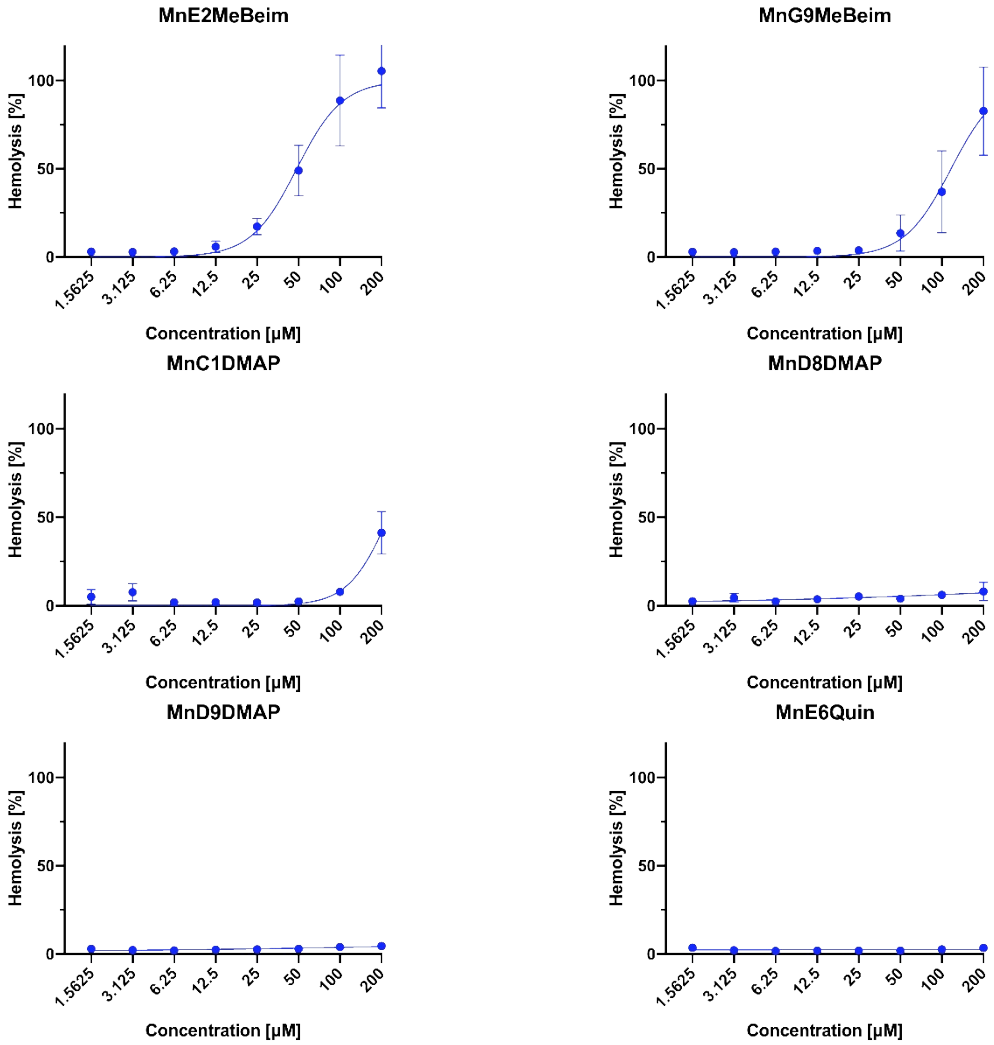

Figure S17. Hemolysis of the HRB cells against different concentration of Mn complex.

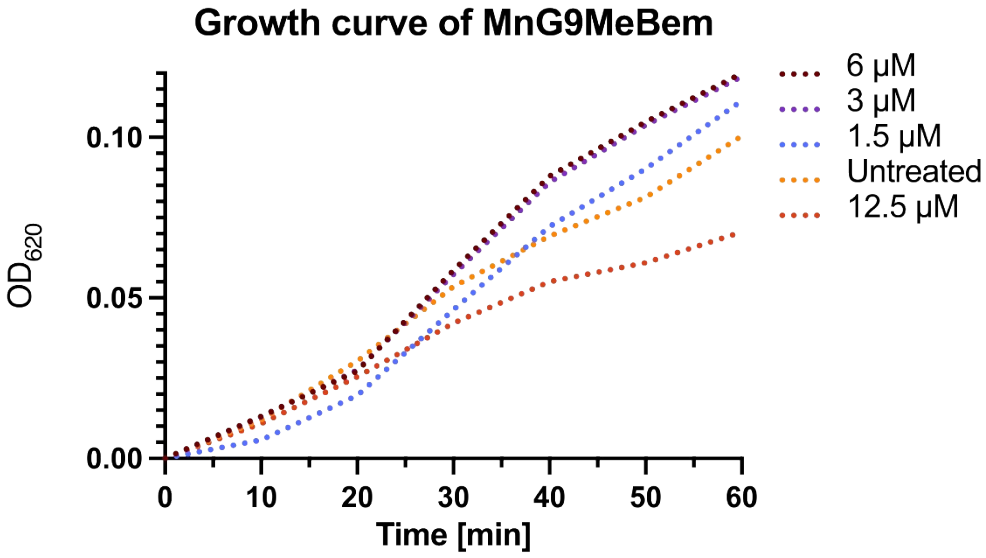

Figure S18. Growth curves of *B. subtilis* in presence of different concentrations of **MnG9MeBeIm** measured at 620 nm over time.

Part 2: Materials and Methods

Physical Measurements.

Analytical RP-HPLC−MS was performed with an Ultimate 3000 Rapid Separation LC−MS System (DAD-3000RS diode array detector) using an Acclaim RSLC 120 C18 column (2.2 µm, 120 Å, 3 × 50 mm, flow 1.2 mL/min) from Dionex. The HPLC is directly linked to a Thermo Scientific LCQ- Fleet Ion-trap MS. The elution solutions were A: MilliQ deionized water containing 0.05% TFA and D: MilliQ deionized water/acetonitrile (10:90,v/v) containing 0.05% TFA. High resolution mass spectra were recorded from LTQ Orbitrap XL with nano ESI (Thermo) positive mode, samples prepared in acetonitrile. NMR were recorded from AVANCE II 400 MHz (Bruker). The FT-IR measurements were recorded on Jasco FT/IR-4700 in the 2500-400 cm^{-1} range, equipped with the UATR accessory. UV-vis spectra were collected using 1 cm quartz cuvette at room temperature with a Shimadzu UV-1800 UV spectrophotometer.

Materials and Reagents.

Reagents were commercially available, and they were used without any further purification.

Combinatorial Synthesis.

Stock solutions of the amines, aldehydes, and axial ligands where prepared at 40 mM in THF. Manganese(I) was activated according previously reported methods.[1] Briefly, bromopentacarbonylmanganese(I) (100 mg, 0.36 mmol) and silver triflate (93.5 mg, 0.36 mmol) were dried with three cycles of vacuum and argon flux. Then, 6 mL of dry THF were added. The suspension then was stirred and refluxed under argon for 45 min. The suspension was then filtered off to get rid of AgBr, and the solution is diluted 1:3 to obtain a 20 mM stock solution in dry THF. The reactants stock solution were combined in a 500 µL Eppendorf vial (50 µL of the amine, 50 µL of the aldehyde, 50 µL of the axial ligand and 100 µL of the Mn(I)), and heated at 75 °C for 2 hours in a water bath.[2] The reaction solution were evaporated under vacuum and dissolved with 100 µL of DMSO to obtained the stock solution at 20 mM. LC-MS was carried out diluting the stock solutions in DMSO in a mixture of ACN:water (50:50) (flux 1.2 $mLmin^{-1}$; A= H_2O 0.1%TFA, D=90%ACN 10% H_2O, 0.1% TFA; program: A/D 100:0 to 0:100 in 5.00 min, total absorbance).

Combinatorial Synthesis Set-up.

All procedures were conducted manually using a standard pipette with a capacity of 20-200 µL. The 70 Eppendorf tubes were arranged in a 96-well plate, and the stock solutions of the compounds were added sequentially—first the aldehyde, followed by the amine, then (if applicable) the axial ligand, and lastly the manganese(I). After the additions, the Eppendorf tubes were sealed with their lids and placed in a floating rack, ensuring that half of the tubes were immersed in the bath. Following the reaction, the vials were transferred directly from the bath to a vacuum chamber to remove the THF. The dried compounds were subsequently dissolved in 100 µL of DMSO and then transferred to a 96-well plate made of polypropylene (PP) in their corresponding positions. From here, the compounds were directly diluted to the working solution for biological activity or LC-MS analysis.

As part of the workflow, the preparation of stock solutions (weighing the compounds and dissolving them in the appropriate solvent) were carried out during the activation of the manganese precursor, taking approximately 2 hours in total. Subsequently, the reaction setup, including the transfer of the solution into the corresponding Eppendorf tubes, was carried out immediately after, requiring approximately 30 minutes. The actual reaction time was 90 minutes, followed by a 3-hour period during which the reaction was left under vacuum. The time required for redissolving the compounds and preparing the stock solution ranged from 30 to 60 minutes. Therefore, the total time for preparing the stock solutions, conducting the reactions, and post-reaction processing for all 70 compounds was approximately 8 hours or one working day.

Batch Synthesis.

Manganese pentacarbonyl bromide (100 mg 0.36 mmol) and silver triflate (93.5 mg, 0.36 mmol) were dried under vacuum. Then 5 mL of dry THF are added and reflux under stirring and under argon atmosphere for 45 min. The suspension was then filtered off. The corresponding amines, aldehydes, and axial ligands (0.072 mmol) are dissolved in 1 mL of the solution of manganese(I) (0.072 mmol). The reaction is headed at reflux under argon for 2 hours. The product is precipitate with 5 mL of heptane, the solid collected, washed with diethylether and dry under vacuum. The pure product is obtained after purification of prepHPLC (flux 40mLmin^{-1}; A= H_2O 0.1%TFA, D=90%ACN 10% H_2O, 0.1% TFA; program: time 0 min A/D 100:0, 5 min A/D 70:30, time 45 min A/D 30-70. For DMAP derivatives A= H_2O, D=100% ACN; program: 0 min A/D 100:0, 5 min A/D 75:25, time 60 min A/D 40-60). The fractions are collected,

checked by LC-MS ((flux 1.2 mLmin^{-1}; A= H_2O 0.1%TFA, D=90%ACN 10% H_2O, 0.1% TFA; program: A/D 100:0 to 0:100 in 10.00 min, total absorbance) and lyophilised.

Mn**C5**MeIm. Yield 45% (22.8 mg). MW 704.49 gmol^{-1}. HR-MS (+, m/z, [M-TfO]$^+$) $[C_{27}H_{21}FMnN_4O_5]^+$ calculated: 555.0876; found: 555.0859. Analytical RP-HPLC: t_R = 4.90 min. ESI-MS (+, m/z, [M-TfO-3CO]$^+$): 470.9 $[C_{24}H_{21}FMnN_4O_2]^+$. ^{1}H NMR (300 MHz, CD_3CN) δ 8.87 (1H, s), 8.39-8.19 (4H, br), 7.89 (1H, m), 7.76-7.59 (2H, br), 7.45-7.35 (5H, br), 7.15-7.06 (1H, m), 6.39 (1H, br), 3.93 (3H, s), 3.68 (3H, br). ^{13}C NMR (400 MHz, CD_3CN) 171.8, 166.5, 165.5, 164.4, 163.8, 163.0, 162.5, 161.9, 148.2, 142.0, 140.7, 134.1, 131.7, 131.6, 130.2, 129.9, 124.5, 123.8, 117.3, 117.1, 52.7, 34.8. IR (ATR): 2033 cm^{-1}, 1931 cm^{-1} v CO.

.

Mn**A3**Clo. Yield 28% (18.0 mg). MW 893.18 gmol^{-1}. HR-MS (+, m/z, [M-TfO]$^+$): $[C_{38}H_{29}ClMnN_4O_5S]^+$ calculated: 743.0928; found: 743.0909. Analytical RP-HPLC: t_R = 5.54 min. ESI-MS (+, m/z, [M-TfO-3CO]$^+$): 658.8 $[C_{35}H_{29}ClMnN_4O_2S]^+$. ^{1}H NMR (400 MHz, DMSO-d_6) δ 8.50 (1H, s), 8.14 (1H, s), 7.50 (1H, m), 7.44 (1H, m) 7.33-7.31 (2H, m), 7.05 (1H, m), 6.68-6.65 (4H, m), 6.69-6.52 (7H, m), 6.28 (1H, s), 6.18-6.18(7H, m), 2.42 (3H, s). ^{13}C NMR (400 MHz, DMSO-d_6) δ 170.6, 153.8, 140.6, 139.8, 139.5, 139.1, 138.7, 137.7, 131.5, 130.3, 130.0, 129.6, 129.2, 129.0, 128.7, 128.5, 128.4, 127.8, 127.8, 127.4, 126.5, 123.2, 121.9, 75.9, 42.0. IR (ATR): 2037 cm^{-1}, 1932 cm^{-1} v CO.

Mn**C8**MeBeim. Yield 30% (16.2 mg). MW 750.58 gmol^{-1}. HR-MS (+, m/z, [M-TfO]$^+$): $[C_{32}H_{26}MnN_4O_5]^+$ calculated: 601.1284; found: 601.1266. Analytical RP-HPLC: t_R = 5.51 min. ESI-MS (+, m/z, [M-TfO-3CO]$^+$): 517.0 $[C_{29}H_{26}MnN_4O_2]^+$. ^{1}H NMR (300 MHz, CD_3CN) δ 9.02 (1H, br), 8.33 (2H, br), 8.08 (1H, br), 7.88-7.85 (1H, d), 7.76-7.65 (3H, m), 7.55 (2H, t), 7.43 (2H, t), 7.35-7.29 (3H, br), 7.12 (2H, br), 3.87 (4.5H, m), 3.41 (1.5H, br), 2.39 (3H, s).. ^{13}C NMR (400 MHz, CD_3CN) δ 171.4, 167.1, 166.2, 165.9, 162.1, 161.1, 159.3, 155.4, 149.6, 146.3, 141.8, 140.8, 140.5, 139.0, 138.8, 131.7, 131.5, 130.7, 130.6, 130.5, 130.1, 125.2, 124.6, 122.1, 121.9, 112.6, 52.6, 32.5, 20.7. IR (ATR): 2029 cm^{-1}, 1918 cm^{-1} v CO.

Mn**C9**MeBeim. Yield 28% (16.4 mg). MW 815.45 gmol^{-1}. HR-MS (+, m/z, [M-TfO]$^+$): $[C_{31}H_{23}BrMnN_4O_5]^+$ calculated: 665.0232; found: 665.0206. Analytical RP-HPLC: t_R =

5.68 min. ESI-MS (+, m/z, [M-TfO-3CO]$^+$): 581.0 [$C_{28}H_{23}BrMnN_4O_2$]$^+$. ^{1}H NMR (300 MHz, CD3CN) δ 9.04 (1H, s), 8.36-8.24 (3H, br), 8.08 (1H, d), 7.88 (1H, d), 7.76-7.53 (7H, m), 7.46-7.35 (2H, m), 7.13 (2H, br), 3.95-3.87 (4.5H, m), 3.41 (1.5H, s). ^{13}C NMR (400 MHz, CD_3CN) δ 172.7, 171.4, 166.0, 151.6, 150.9, 146.3, 142.4, 141.7, 140.9, 134.1, 133.3, 133.2, 132.0, 131.6, 131.5, 130.5, 130.4, 130.1, 128.7, 125.3, 124.6, 124.2, 124.0, 112.6, 52.6, 32.5. IR (ATR): 2031 cm^{-1}, 1923 cm^{-1} ν CO.

Mn**E2**MeBeim. No prepHPLC needed. Compound pure after precipitation and washing. Yield 99% (48.9 mg). MW 686.47 gmol^{-1}. HR-MS (+, m/z, [M-TfO]$^+$) [$C_{28}H_{19}F_3MnN_4O_4$]$^+$ calculated: 587.0739; found: 587.0718. Analytical RP-HPLC: t_R = 5.74 min. ESI-MS (+, m/z, [M-TfO-3CO]$^+$): 503.1 [$C_{25}H_{19}F_3MnN_4O_1$]$^+$. ^{1}H NMR (300 MHz, CD_3CN) δ 9.42 (1H, s), 8.85 (1H, s), 8.47-8.44 (1H, d), 8.31-8.28 (1H, d), 7.84-7.79 (4H, m), 7.63-7.60 (1H, m), 7.48-7.45 (1H, m), 7.39 (1H, m), 7.32 (1H, d), 7.29 (1H, s), 6.73 (1H, s), 3.73 (3H, s). ^{13}C NMR (400 MHz, CD_3CN) δ 171.5, 154.7, 152.7, 150.7, 149.1, 146.9, 146.1, 142.8, 135.5, 133.7, 132.5, 131.6, 127.6, 127.6, 125.1, 124.4, 123.5, 118.6, 113.8, 113.1, 112.3, 32.3. IR (ATR): 2033 cm^{-1}, 1934 cm^{-1} ν CO.

Mn**G9**MeBeim. Yield 26% (14.5 mg). MW 778.21 gmol^{-1}. Anal. calcd for $C_{23}H_{15}Br_2FMnN_4O_3 \cdot C_4HF_5O_4$ (%): C, 37.88; H, 1.88; N, 6.54. Found: C, 38.61; H, 1.88; N, 6.39. HR-MS (+, m/z, [M-TfO]$^+$): [$C_{23}H_{15}Br_2FMnN_4O_3$]$^+$ calculated: 626.8875; found: 626.8860. Analytical RP-HPLC: t_R = 5.42 min. ESI-MS (+, m/z, [M-TfO-3CO]$^+$): 544.1 [$C_{20}H_{15}Br_2FMnN_4$]$^+$. ^{1}H NMR (300 MHz, CD_3CN) δ 8.92 (1H, s), 8.15 (1H, br), 7.90 (1H, br), 7.77-7.75 (2H, d), 7.70-7.65 (2H, t), 7.52-7.47 (2H, t), 7.43-7.41 (1H, d), 7.38-7.32 (2H, m), 3.81 (3H, s). ^{13}C NMR (400 MHz, CD_3CN) δ 166.8, 150.7, 147.0, 142.5, 138.0, 137.9, 135.4, 133.5, 133.2, 132.9, 125.2, 124.7, 124.6, 124.5, 124.0, 123.7, 112.5, 32.4. IR (ATR): 2034 cm^{-1}, 1923 cm^{-1} ν CO. XRD: CCDC No 2280008.

Mn**C1**DMAP. Yield 29% (15.4 mg). MW 740.59 gmol^{-1}. HR-MS (+, m/z, [M-TfO]$^+$) [$C_{32}H_{30}MnN_4O_7$]$^+$ calculated: 637.1495; found: 637.1478. Analytical RP-HPLC: t_R = 5.35 min. ESI-MS (+, m/z, [M-TfO-3CO]$^+$): 553.1 [$C_{29}H_{30}MnN_4O_4$]$^+$. ^{1}H NMR (300 MHz, CD_3CN) δ 8.85 (1H,br), 8.24-7.76 (9H, m and br), 7.34 (2H. br), 7.10 (2H, br), 6.50 (2H, br), 3.89 (6H, br), 2.96 (3H, br), 1.94 (6H, br). ^{13}C NMR (400 MHz, CD_3CN) δ 169.7, 166.5, 158.2, 155.8, 151.6, 150.9, 150.3, 145.1, 144.8, 141.8, 140.7, 131.9,

131.7, 131.1, 130.3, 129.3, 112.3, 109.0, 106.7, 56.3, 52.7, 39.0. IR (ATR): 2027 cm^{-1}, 1916 cm^{-1} v CO. XRD: CCDC No 2280009.

Mn**D8**DMAP. No prepHPLC needed. Yield 64% (31.8 mg). MW 689.59 $gmol^{-1}$. HR-MS (+, m/z, $[M\text{-}TfO]^+$) $[C_{28}H_{31}MnN_5O_3]^+$ calculated: 540.1807; found: 540.1790. Analytical RP-HPLC: t_R = 6.30 min. ESI-MS (+, m/z, $[M\text{-}TfO\text{-}3CO]^+$): 456.1 $[C_{28}H_{31}MnN_5O_3]^+$. ^1H NMR (300 MHz, CD_3CN) δ 8.70 (1H, s), 8.06 (1H, m), 7.66-7.59 (2H, m), 7.48 (m, 4H), 7.33 (2H, m), 6.46 (2H, m), 3.50 (2H, br), 3.21-3.05 (4H, br), 2.95 (6H, s), 2.49 (3H, s), 1.88 (2H, br),1.75 (2H, br). ^{13}C NMR (400 MHz, CD_3CN) δ 170.6, 169.8, 155.0, 153.0, 151.4, 149.2, 141.7, 140.6, 131.0, 125.0, 122.7, 121.7, 108.7, 39.1, 39.0, 24.6, 24.0, 20.7. IR (ATR): 2024 cm^{-1}, 1924 cm^{-1} v CO. XRD: CCDC No 2280010.

Mn**D9**DMAP. Yield 29% (15.8 mg). MW 754.46 $gmol^{-1}$. HR-MS (+, m/z, $[M\text{-}TfO]^+$) $[C_{27}H_{28}BrMnN_5O_3]^+$ calculated: 604.0756; found: 604.0740. Analytical RP-HPLC: t_R = 6.38 min. ESI-MS (+, m/z, $[M\text{-}TfO\text{-}3CO]^+$): 522.0 $[C_{24}H_{28}BrMnN_5]^+$. ^1H NMR (300 MHz, CD_3CN) δ 8.71 (1H, s), 8.08 (1H, t), 7.82 (2H, d), 7.69-7.62 (2H, m), 7.49 (2H, d), 7.32 (2H, d), 6.45 (2H, d), 3.64-3.22 (5H, br), 2.95 (6H, s),1.87-1.65 (5H, br). ^{13}C NMR (400 MHz, CD_3CN) δ 171.9, 169.9, 155.3, 154.8, 151.4, 150.5, 141.8, 137.9, 133.7, 125.5, 124.8, 123.2, 122.2, 108.8, 39.0, 24.6, 24.0. IR (ATR): 2028 cm^{-1}, 1919 cm^{-1} v CO.

Mn**E6**Quin. Yield 34% (18.3 mg). MW 747.53 $gmol^{-1}$. HR-MS (+, m/z): $[M\text{-}TfO]^+$/ $[C_{32}H_{21}MnN_3O_6]^+$ calculated: 598.0811; found: 598.0800; $[M\text{-}TfO\text{-}3CO+MeOH]^+$/ $[C_{30}H_{25}MnN_3O_4]^+$ calculated: 546.1226; found: 598.0848. Analytical RP-HPLC: t_R = 5.35 min. ESI-MS (+, m/z, $[M\text{-}TfO\text{-}3CO]^+$): 514.1 $[C_{29}H_{21}MnN_3O_3]^+$. ^1H NMR (300 MHz, CD_3CN) δ 9.56 (1H, s), 8.76 (1H, s), 8.61 (1H, s), 8.32 (1H, d), 8.00 (1H, d), 7.92 -7.84 (4H, m), 7.78-7.75 (2H, m), 7.67-7.61(2H, m), 7.41 (1H, d), 7.32 (1H, d), 7.25 (1H, s), 6.69 (1H, s), 6.34 (1H), 2.44 (3H, s). ^{13}C NMR (400 MHz, CD_3CN) δ 171.4, 157.5, 154.9, 153.4, 153.2, 152.8, 150.7, 149.1, 147.0, 145.0, 136.6, 134.0, 133.9, 132.8, 131.2, 129.8, 129.7, 128.7, 127.6, 127.0, 123.8, 121.4, 119.6, 116.2, 114.0, 113.5, 111.1, 18.4. IR (ATR): 2037 cm^{-1}, 1941 cm^{-1} v CO.

Crystallographic data collection and crystal structure determination

Single crystal X-ray diffraction analyses were carried out with a Bruker D8Venture diffractometer equipped with a kappa goniometer and an Oxford cryosystem. Microfocused MoKα radiation (λ = 0.71073) was used and Lorentz polarization and absorption correction were applied by the SADABS[3] procedure. The phase problem was solved by direct methods and the structures were refined by full-matrix least-squares on all F2 using SHELXL[4,5], as implemented in the OLEX2 suite of programs. Analytical expressions of neutral atom scattering factors were taken from the International Tables for X-Ray Crystallography[6]. The structure drawings were obtained using ORTEPIII[7] and Mercury[8]. CCDC 2280008-2280010 contain the supplementary crystallographic data. These data can be obtained free of charge via http://www.ccdc.cam.ac.uk/conts/retrieving.html. X-Ray structure determination analysis were performed on crystals grown by recrystallization from the solvent (EtOH for **MnD8DMAP**, MeOH for **MnC1DMAP**, THF in diffusion with heptane for **MnG9MeBeIm**).

UV-vis spectroscopy

UV-vis spectra were collected using 1 cm quartz cuvette at room temperature. Stock solution of the complexes were 5 mM in DMSO and were diluted in DMSO or PBS to 50 μM finial concentration. Stability was checked by following the maximum of absorption during 18 hours of incubation with a plate reader (Tecan instrument Infinite M1000).

The release of carbon monoxide (CO) from metal carbonyl complexes was assessed spectrophotometrically by measuring the conversion of hemoglobin (Hb) to carboxyhemoglobin (Hb-CO) adapting a previously published procedure.[9] Briefly, fresh solutions of hemoglobin with a final concentration of 80 μM were prepared by dissolving the protein in HEPES pH 7.4. Prior to each reading, a freshly prepared solution of sodium dithionite (0.1%) was added to convert hemoblogin to deoxyhemoglobin. After preparing the myoglobin solutions, a stock solution of **MnG9MeBeIm** was added to achieve a final concentration of 20 μM. The absorbance was then measured from 500 nm to 650 nm at 30-minute intervals over a duration of 8 hours.

Identification of active compounds and MIC and MBC determination.

The samples were tested for their antimicrobial activity against *Escherichia coli* W3110, *Staphylococcus aureus* COL (MRSA), *Pseudomonas aeruginosa* PAO1, *Acinetobacter baumannii* ATCC19606, *Klebsiella pneumoniae* NCTC418, and methicillin-resistant *Staphylococcus aureus* COL, clinical isolate *Staphylococcus epidermidis*, clinical isolate methicillin susceptible *Staphylococcus aureus*, *Bacillus subtilis* 168 CA (wild type), *Enterococcus spp* S342, *Enterococcus casselliflavus* S9. *Enterococcus* clinical isolate strains isolated in the laboratory of Food Inspection Unit of Parma University from pig food chain. Resistance to vancomycin was verified by VanA detection by PCR. A colony of bacteria was grown in Luria-Bertani (LB) medium overnight at 37 °C. Stock solutions of 2 mM of the samples were prepared in DMSO and diluted to a starting concentration of 100 μM in Mueller Hinton (MH) medium. For the identification of the active compound only one concentration (100 μM) was used, for the MIC determination the samples were two folds diluted. The bacteria concentration was measured by measuring the optical density at 600 nm and diluted to OD_{600} of 0.022 in MH medium. 5 μL of the diluted bacterial solution was used to

inoculate 150 µL of the sample solutions, resulting in a final inoculation of about 5 × 10^5 CFU/mL. The plates were then incubated at 37 °C for 18 hours. For each assay, a control of broth only and a growth control of broth with bacterial inoculum without antibiotics were included in two columns of the plate. Polymyxin B and Vancomycin were used as control antibiotic for *E. coli* and MRSA respectively. The growth was measured by analysing the absorbance of the bacterial suspension at 600 nm using a plate reader (Tecan instrument Infinite M1000). The MBC values were determined by resuspending 10 µL of the suspension from the MIC plate in fresh LB agar. After 18 hours, the agar plates were checked and the MBC was determined as the concentration that could prevent the re-growth of any bacteria.

A competitive assay with hemoglobin was conducted by preparing different MH media (with 160, 80, 40, 20, 10, 5, 2.5 µM). This was achieved by adding a stock solution of hemoglobin in PBS, which was sterilized through filtration. The FICI values were determined as follows: $FICI=FIC_A+FIC_B=C_A/MIC_A+C_B/MIC_B$, where MIC_A and MIC_B are the MIC values of compounds A and B alone, and C_A and C_B are the effective concentration of A and B when administrated. A FICI index of 0.5 or less indicates synergistic effect; between 0.5 and 4 the effect is additive. FICI index greater than 4 denotes antagonism.[10,11]

Haemolysis assay.

The compounds were tested on human red blood cells (hRBCs) using a haemolysis assay as previously reported.[12] Blood was obtained from Interregionale Blutspende SRK AG in Bern, Switzerland. 1.5 mL of whole blood was centrifuged at 3000 rpm for 15 minutes at 4 °C, and the plasma was discarded. The hRBC pellet was washed three times with PBS (pH 7.4) and then resuspended to a final volume of 10 mL in PBS. For the identification of the not haemolytic compound only one concentration (20 µM) was used, for the determination of HC_{50} of the lead compounds, the samples were two folds diluted starting from 200 µM. Samples stock solution was 20 mM in DMSO. Each plate included a blank medium control (PBS) and a haemolytic activity control (0.1% Triton TM X-100). hRBC suspension was incubated with the samples in PBS in a V-shaped 96-well plate for 4 hours at 20 °C. After the incubation, 100 µL of supernatant was carefully pipetted to a flat bottom, clear 96-wells plate. Haemolysis was measured by analysing the absorbance of free haemoglobin in the supernatants

at 540 nm using a plate reader (Tecan instrument Infinite M1000). The percentage of haemolysis at each concentration was determined and the HC_{50} was calculated. The growth was measured by analysing the absorbance of free hemoglobin in the supernatants at 540 nm using a plate reader (Tecan instrument Infinite M1000).

Cytotoxicity.

The HuDe human epithelial cells were purchased from the American Type Culture Collection (ATCC, Manassas, VA, USA). The cells were cultivated in RPMI 1640 medium supplemented with 10% heat-inactivated fetal bovine serum, 100 UmL^{-1} of penicillin and streptomycin, and maintained at a temperature of 37 °C with 5% CO_2. All experiments were carried out using cells that were in the log phase. Initially, 100 000 mL^{-1} of cells were seeded into 96-well plates and incubated for 18-24 hours before being exposed to compounds at concentrations ranging from 0.1 µM to 100 µM. Following a 24 hour incubation period at 37 °C, the cells were stained with Trypan Blue and counted using a haemocytometer. The control for the experiments was DMSO. Each sample was tested in at least three independent experiments. The concentration of a compound required to reduce cell growth by 50% compared to untreated control cells was determined as the half maximal inhibitory concentration (IC_{50}).

Bacterial Growth Curve.

An overnight culture of *Bacillus subtilis* was grown in 20 mL of Luria-Bertani (LB) medium in an Erlenmeyer flask until reaching an optical density of 0.3 under agitation. The bacterial suspension was subsequently distributed into a 24-well plate. The complex **MnG9MeBeIm** was added at concentrations of 12.5, 6, 3, and 1.5 µM. Absorbance was monitored at 620 nm using a plate reader for one hour.

Fluorescence light microscopy

Protocols were adapted from previous reported papers.[13] Fluorescence light microscopy was performed using a Nikon Ti-2 Eclipse,Nikon Europe BV, Amsterdam, Netherlands with a CFI Plan Fluor 40× oil immersion objective (CFI Plan Fluor 40×/1.30 W.D. 0.24, Nikon Europe BV). Brightfield and fluorescence images were recorded by an Andor Zyla 4.2 Plus USB3 camera in Widefield and using LED light excitation. Images were analyzed using ImageJ (Fiji). *Bacillus subtilis* PrpsD (MW54)

expressing cytosolic GFP from the strong ribosomal PrpsD promoter was grown in LB at 37 °C under steady agitation in the presence of 100 µg/mL Spectinomycin. *Bacillus subtilis* MinD (KS69) was grown in LB at 37 °C under steady agitation in the presence of 50 µg/mL Spectinomycin. Overnight cultures of *B. subtilis* were regrown in LB (for MinD, 0.1% Xylose as an inducer is needed for the second culture). **MnG9MeBeIm** and controls were added at an OD_{600} of 0.3 and images were taken after 20 min of antibiotic treatment. Cells were immobilized on pre warmed 1.2% agarose-covered slides in HEPES buffer (50 mM pH 7.4)[14]. Membranes were stained with 0.5 µg/mL Nile red for 5 min. Nucleoids were stained with 1 µg/mL DAPI for 5 min. Carbon monoxide release was measured using BioTracker Carbon Monoxide Probe 1 Live Cell Dye (Sigma, SCT051) with the addition of $PdCl_2$ at 5 µM for 20 minutes.

Propidium iodide assay

Permeability for the large fluorescent molecule propidium iodide as a reporter for the presence of large membrane pores or severe membrane disruption was quantified using a Tecan Infinite M1000 plate reader, following the previously described protocol[16,17]. Cells were grown until an OD_{600} of 0.3 and antibiotics were added simultaneously with 13.3 µg/mL propidium iodide (1 mg/mL stock in DMSO). After 15 min, cells were centrifugated and the pallet washed twice with HEPES buffer (pH 7.4) and fluorescence was measured using 535 nm excitation and 617 nm emission wavelengths. SDS 0.05% served as positive control. Each experiment was performed in triplicate.

$DIS_3(5)$ assay

Membrane potential measurements were conducted using the potentiometric fluorescent probe 3,3'-dipropylthiadicarbocyanine iodide (DiSC3(5)) on a Tecan Infinite M1000 plate reader, following the previously described protocol[16,17]. Briefly, 1 µM DiSC3(5) was added to exponentially growing *B. subtilis 168* cultures at 37 °C, and the baseline was recorded for 5 minutes using an excitation wavelength of 651 nm and an emission wavelength of 675 nm. MnG9MeBeIm (3 µM), gramicidin (1 µg/mL, positive control) were then added, and samples were measured for an additional 20 minutes at 37 °C. Each experiment was performed in triplicate.

Resazurin assay

Respiratory chain activity was measured following the reduction of resazurin to resofurin by fluorescence, following the previously described protocol[16,17]. *B. subtilis 168* was cultivated in LB medium at 37 °C until reaching an optical density (OD_{600}) of 0.3. Following that, the cells were treated with different concentrations of MnG9MeBeIm (1.5, 3, 6, 12 µM), 100 µM CCCP, or 15 mM sodium azide. After 15 minutes, samples were collected and adjusted to an OD_{600} of 0.15 through dilution with medium. Subsequently, the samples were incubated for 5 minutes with 100 µg/mL of resazurin under steady agitation at 37 °C. Fluorescence measurements were taken using an excitation wavelength of 545 nm, and the emitted light was recorded at 630 nm. The reported percentages represent the relative values compared to the untreated control. Each experiment was performed with two biological replicates and three technical replicates.

Part 3: Characterization Spectra (HRMS, LCMS, ^{1}H NMR, ^{13}C NMR, IR)

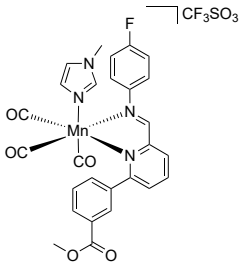

A. Mn**C5**MeIm

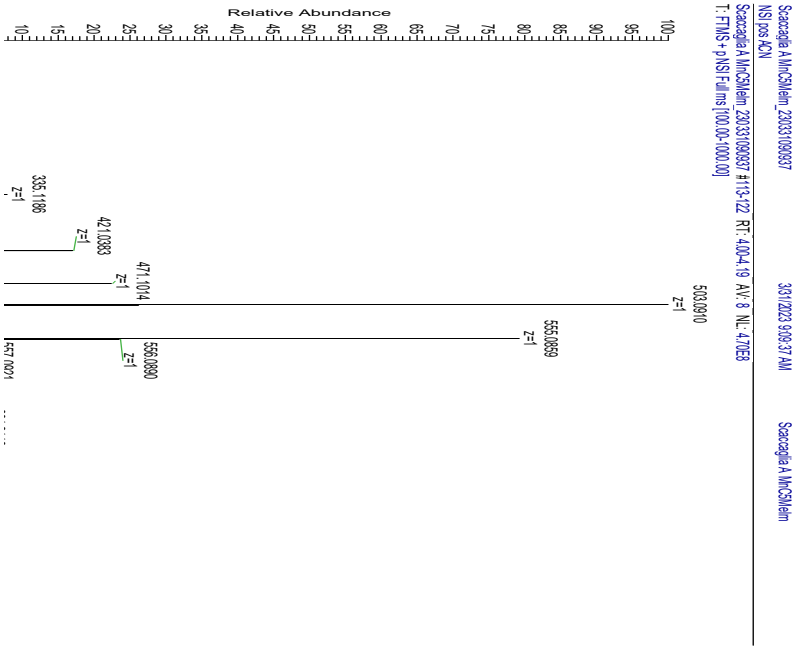

Figure S19. HRMS spectra of MnC5MeIm

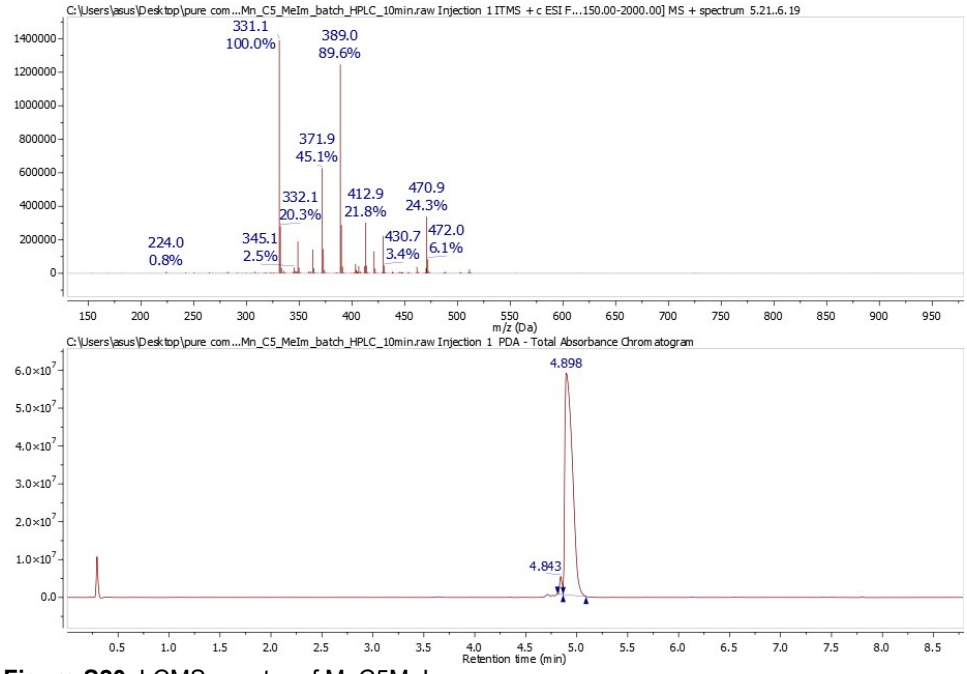

Figure S20. LCMS spectra of MnC5MeIm

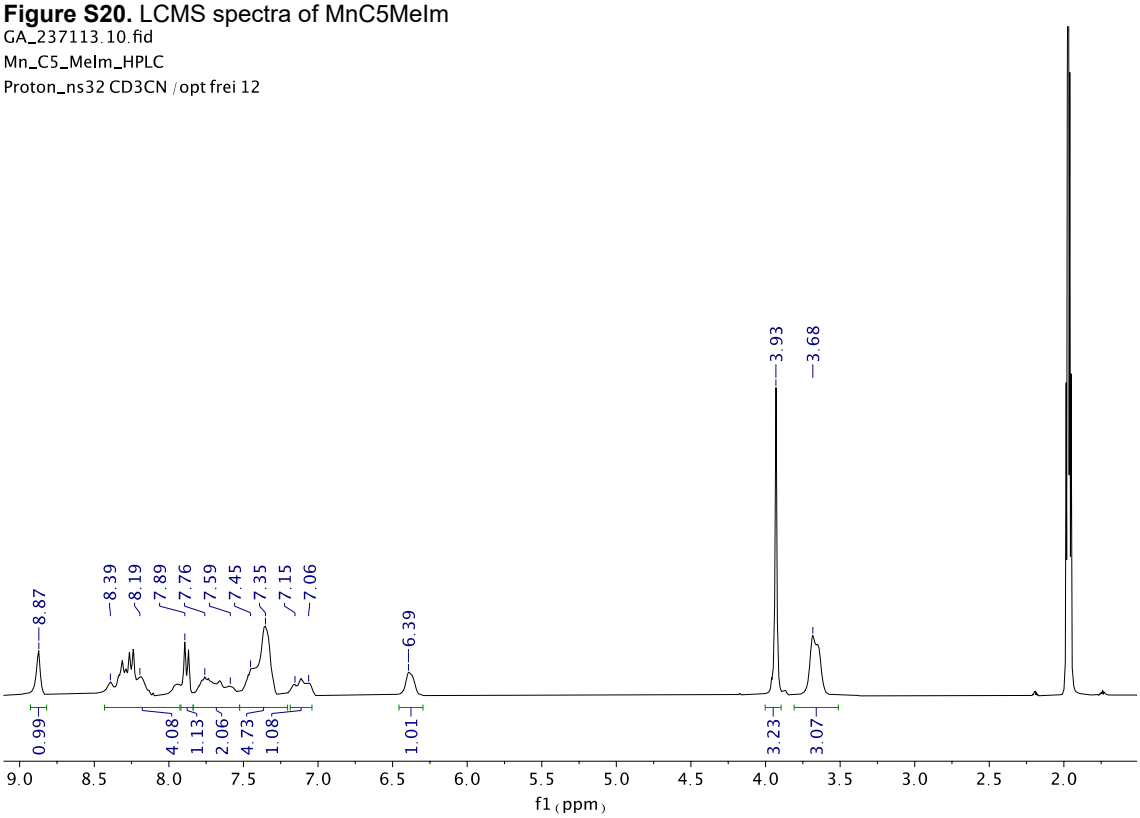

Figure S21. ^{1}H NMR of MnC5MeIm (300 MHz, CD_3CN) δ 8.87 (1H, s), 8.39-8.19 (4H, br), 7.89 (1H, m), 7.76-7.59 (2H, br), 7.45-7.35 (5H, br), 7.15-7.06 (1H, m), 6.39 (1H, br), 3.93 (3H, s), 3.68 (3H, br).

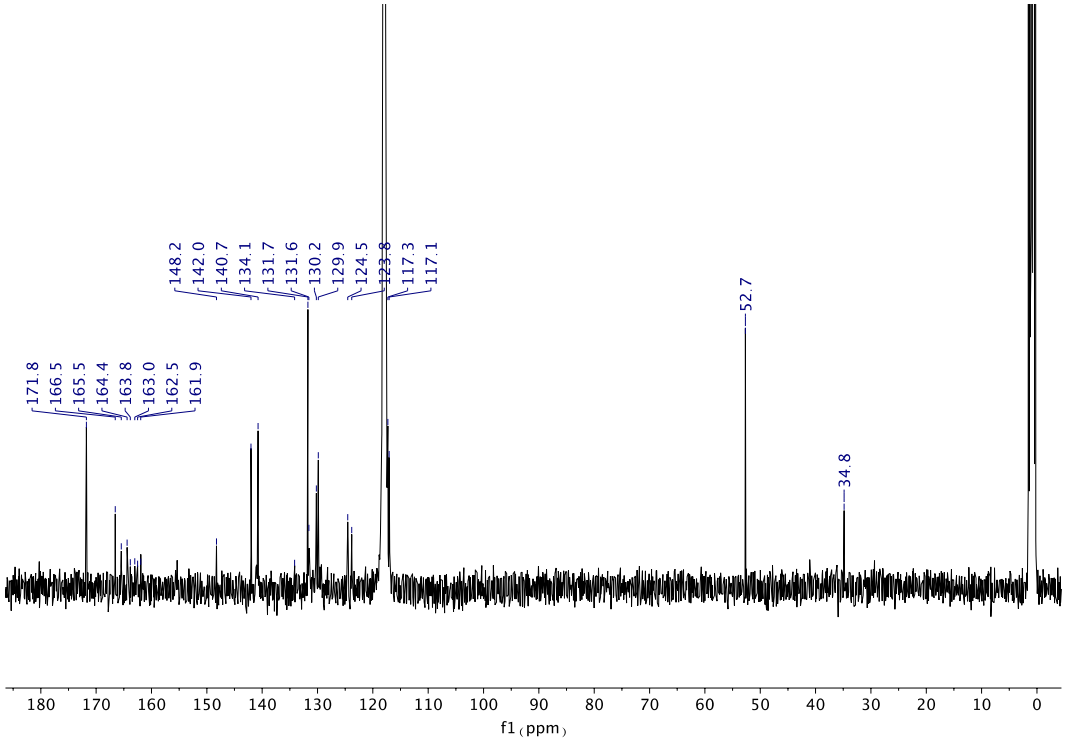

Figure S22. ^{13}C NMR spectra of MnC5MeIm (400 MHz, CD3CN) 171.8, 166.5, 165.5, 164.4, 163.8, 163.0, 162.5, 161.9, 148.2, 142.0, 140.7, 134.1, 131.7, 131.6, 130.2, 129.9, 124.5, 123.8, 117.3, 117.1, 52.7, 34.8.

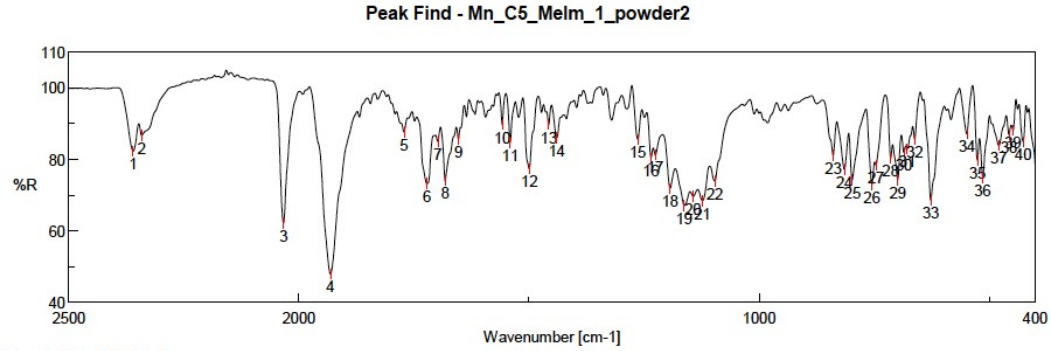

[Result of Peak Picking]

No.	Position	Intensity	No.	Position	Intensity	No.	Position	Intensity
1	2360.44	82.2333	2	2342.12	86.6381	3	2033.57	62.0668
4	1931.36	47.8841	5	1771.3	87.6103	6	1722.12	73.2693
7	1698.02	85.0578	8	1682.59	74.0231	9	1653.66	85.564
10	1558.2	89.6447	11	1540.85	84.6999	12	1499.38	77.2684
13	1456.96	89.6658	14	1439.6	86.0154	15	1264.11	85.5803
16	1235.18	80.3844	17	1225.54	81.176	18	1193.72	71.8789
19	1162.87	67.0693	20	1143.58	69.6173	21	1123.33	68.4371
22	1096.33	73.9402	23	838.883	81.1081	24	814.777	77.1506
25	797.421	74.2653	26	754.995	72.8421	27	746.317	78.3704
28	714.497	80.2851	29	699.069	74.2766	30	685.57	81.8295
31	677.856	82.9565	32	661.464	85.6025	33	626.752	68.5075
34	548.649	87.0726	35	525.507	79.7426	36	513.936	74.8491
37	479.224	83.8289	38	457.047	86.8442	39	448.369	88.1702
40	426.191	84.9609						

Figure S23. IR spectra of MnC5MeIm (ATR): 2033 cm^{-1}, 1931 cm^{-1} v CO

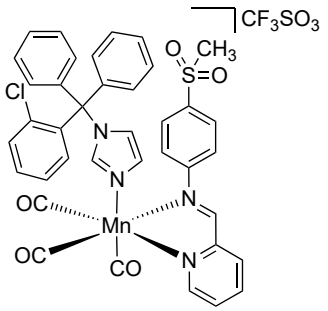

B. Mn**A3**Clo

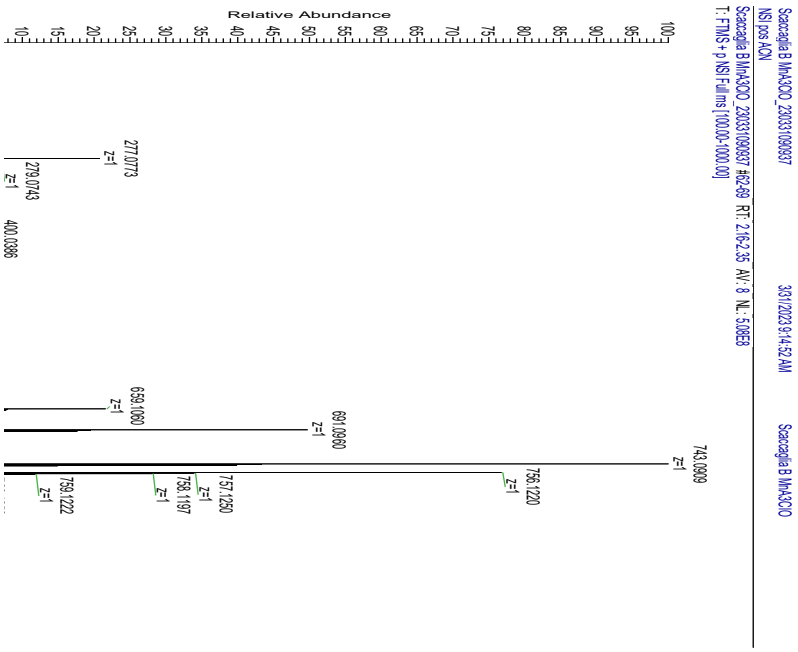

Figure S24. HRMS spectra of MnA3Clo

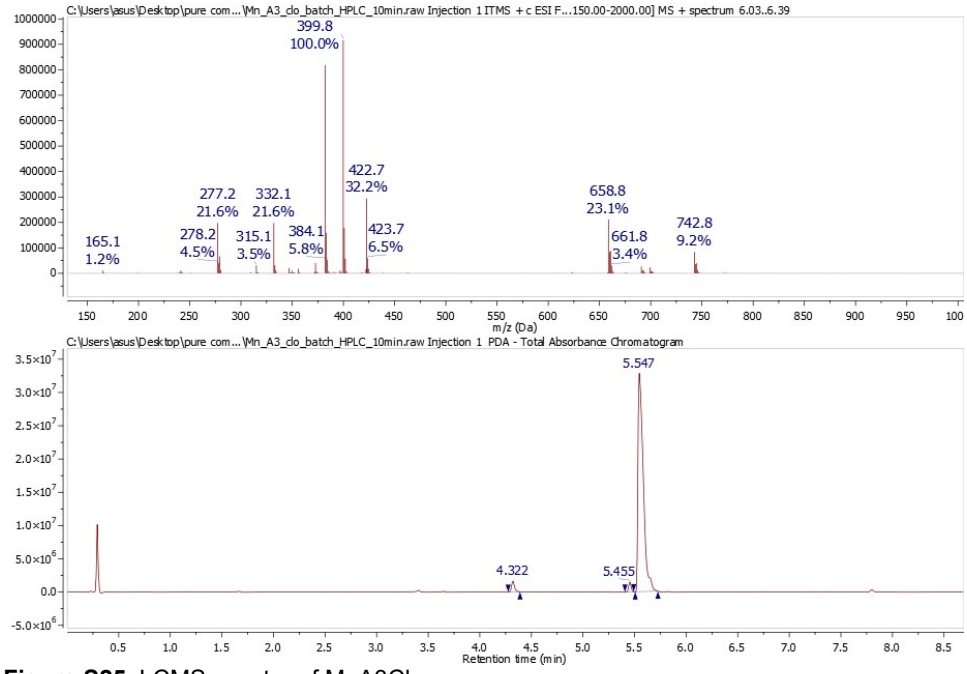

Figure S25. LCMS spectra of MnA3Clo

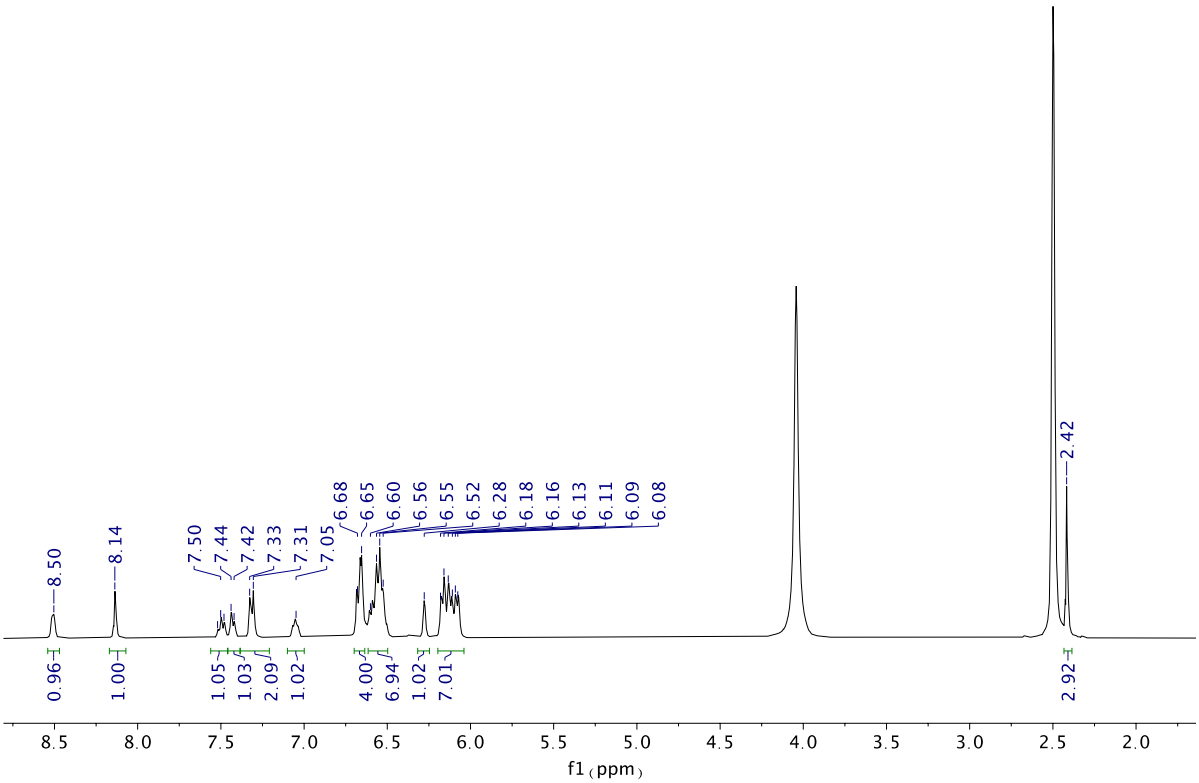

Figure S26. ^{1}H NMR spectra of MnA3Clo (400 MHz, DMSO-d_6) δ 8.50 (1H, s), 8.14 (1H, s), 7.50 (1H, m), 7.44 (1H, m) 7.33-7.31 (2H, m), 7.05 (1H, m), 6.68-6.65 (4H, m), 6.69-6.52 (7H, m), 6.28 (1H, s), 6.18-6.18(7H, m), 2.42 (3H, s).

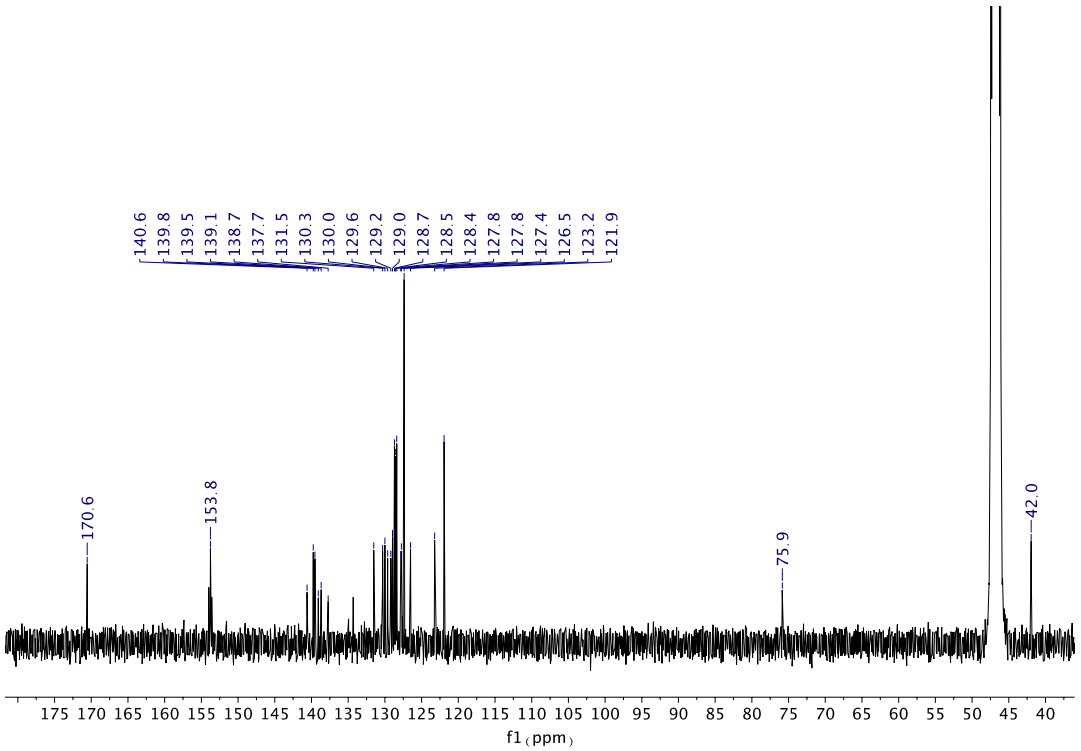

Figure S27. ^{13}C NMR spectra of MnA3Clo (400 MHz, DMSO-d_6) δ 170.6, 153.8, 140.6, 139.8, 139.5, 139.1, 138.7, 137.7, 131.5, 130.3, 130.0, 129.6, 129.2, 129.0, 128.7, 128.5, 128.4, 127.8, 127.8, 127.4, 126.5, 123.2, 121.9, 75.9, 42.0.

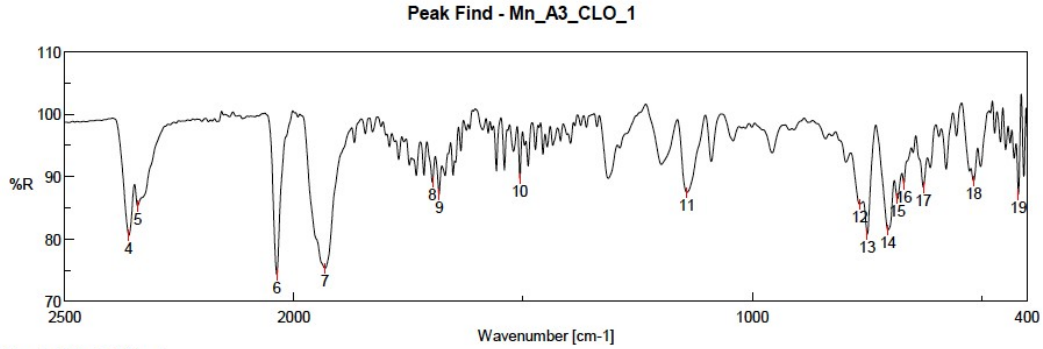

[Result of Peak Picking]

No.	Position	Intensity	No.	Position	Intensity	No.	Position	Intensity
1	3749.9	89.3426	2	3734.48	88.4075	3	3648.66	88.496
4	2360.44	80.5661	5	2341.16	85.3112	6	2037.43	74.2676
7	1932.32	75.3144	8	1698.02	89.0551	9	1683.55	87.1065
10	1507.1	89.6794	11	1142.62	87.4492	12	765.601	85.5862
13	749.209	80.7474	14	703.89	81.4106	15	683.642	86.4511
16	669.178	88.8638	17	626.752	88.2742	18	516.829	89.3206
19	419.442	87.175						

Figure S28. IR spectra of MnA3Clo (ATR): 2037 cm^{-1}, 1932 cm^{-1} ν CO

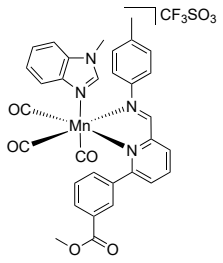

C. Mn**C8**MeBeim

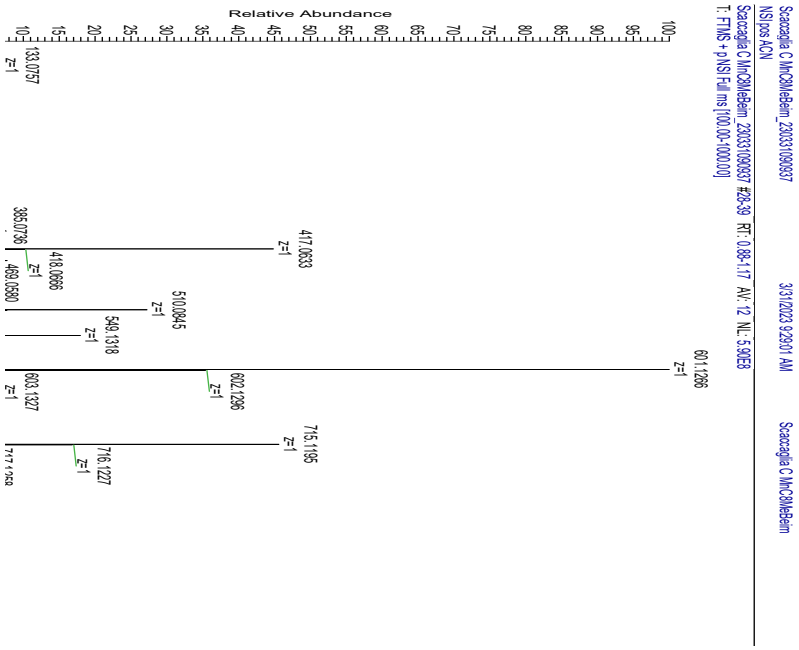

Figure S29. HRMS spectra of MnC8MeBeIm

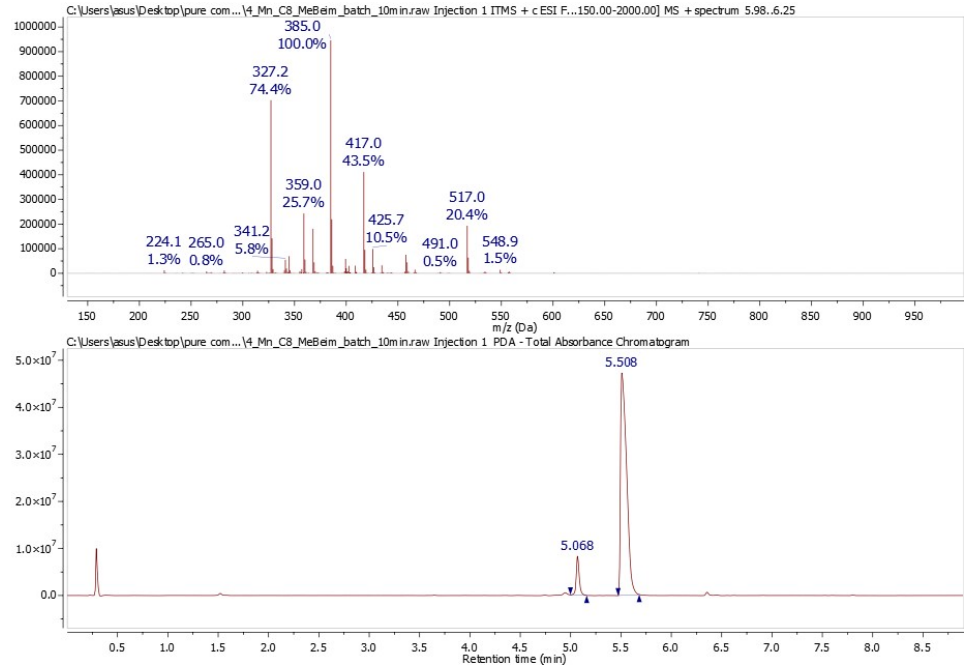

Figure S30. LCMS spectra of MnC8MeBeIm

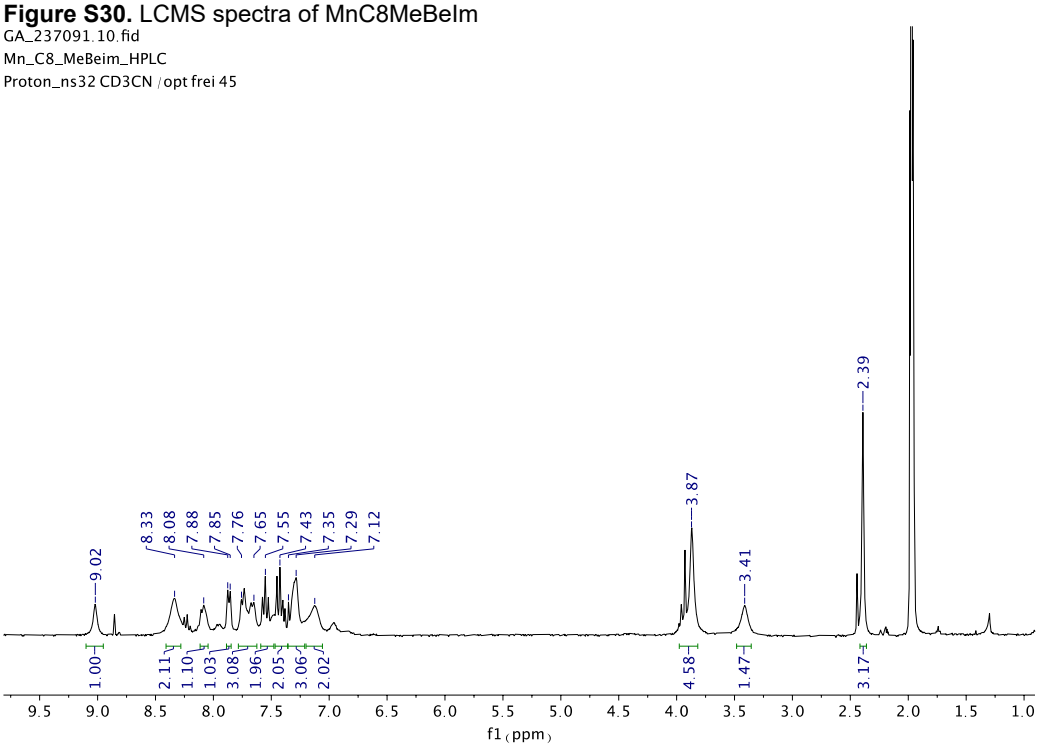

Figure S31. ^{1}H NMR spectra of MnC8MeBeIm (400 MHz, DMSO-d_6) δ 8.50 (1H, s), 8.14 (1H, s), 7.50 (1H, m), 7.44 (1H, m) 7.33-7.31 (2H, m), 7.05 (1H, m), 6.68-6.65 (4H, m), 6.69-6.52 (7H, m), 6.28 (1H, s), 6.18-6.18(7H, m), 2.42 (3H, s).

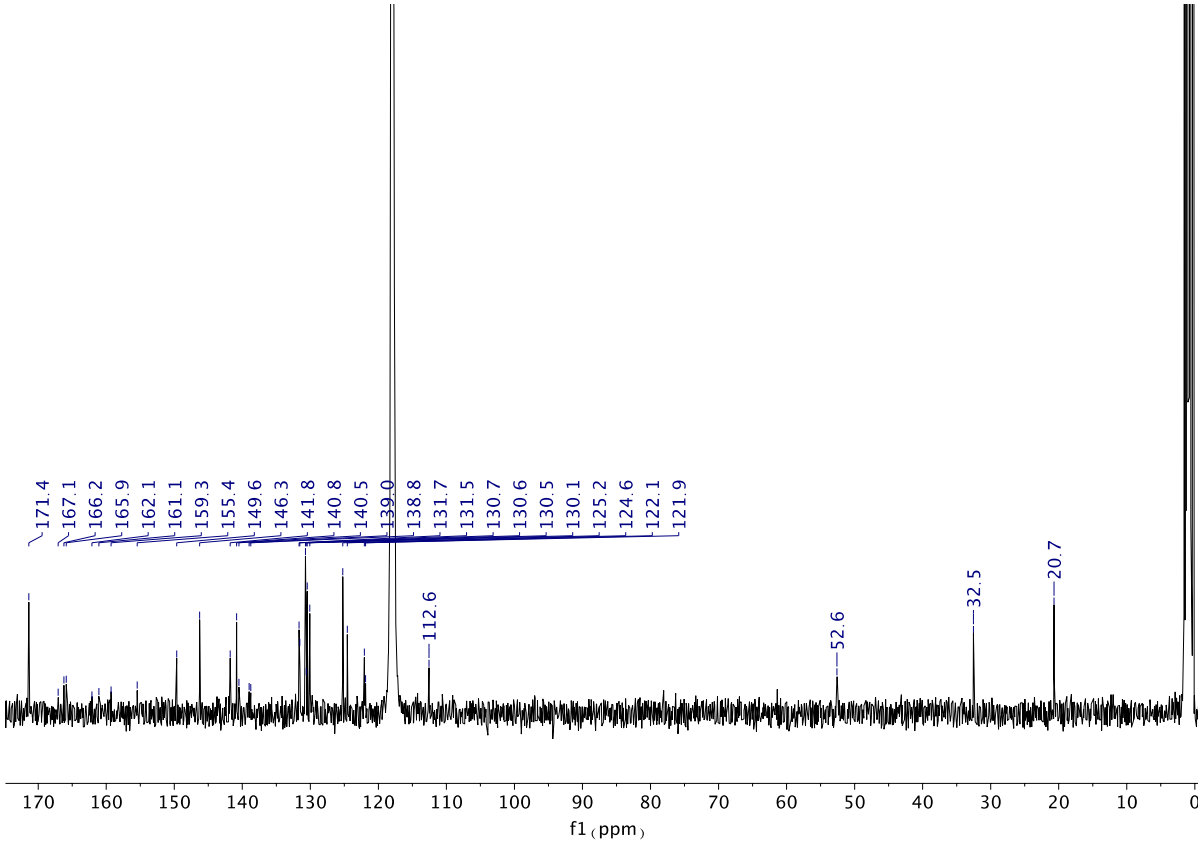

Figure S32. ^{13}C NMR spectra of MnC8MeBeIm (400 MHz, CD3CN) δ 171.4, 167.1, 166.2, 165.9, 162.1, 161.1, 159.3, 155.4, 149.6, 146.3, 141.8, 140.8, 140.5, 139.0, 138.8, 131.7, 131.5, 130.7, 130.6, 130.5, 130.1, 125.2, 124.6, 122.1, 121.9, 112.6, 52.6, 32.5, 20.7.

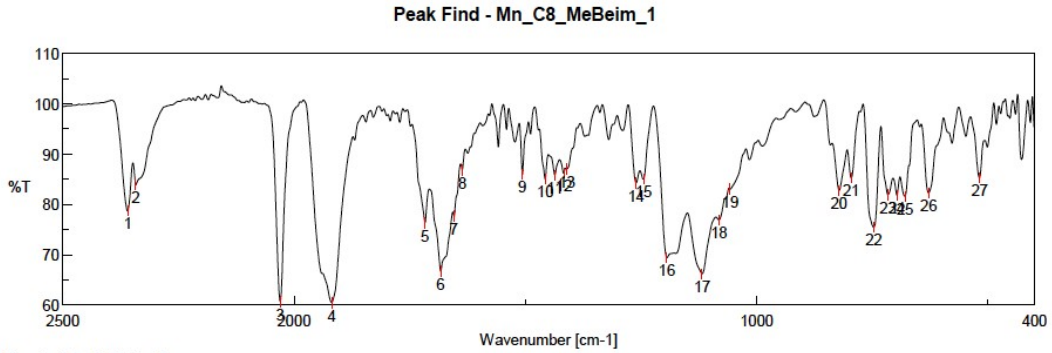

[Result of Peak Picking]

No.	Position	Intensity	No.	Position	Intensity	No.	Position	Intensity
1	2359.48	78.6968	2	2342.12	83.8984	3	2029.71	60.6863
4	1918.82	60.4771	5	1717.3	76.3476	6	1683.55	66.7061
7	1654.62	77.64	8	1636.3	86.8515	9	1507.1	85.9104
10	1456.96	85.0043	11	1436.71	85.7873	12	1417.42	86.2342
13	1410.67	87.053	14	1261.22	84.2734	15	1244.83	85.0059
16	1194.69	69.4086	17	1118.51	66.2228	18	1081.87	76.903
19	1057.76	83.0159	20	822.491	82.7676	21	796.457	85.2258
22	747.281	75.46	23	716.425	81.9152	24	697.141	81.817
25	679.785	81.6078	26	628.68	82.2624	27	518.758	85.2285

Figure S33. IR (spectra of MnC8MeBeIm ATR): 2029 cm^{-1}, 1918 cm^{-1} v CO

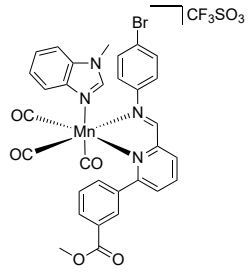

D. Mn**C9**MeBeim

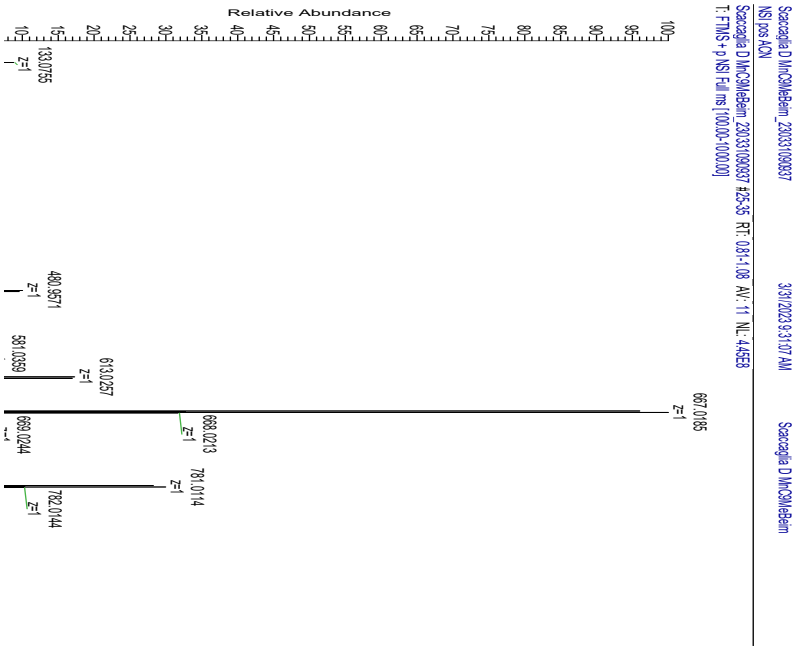

Figure S34. HRMS spectra of MnC9MeBeIm

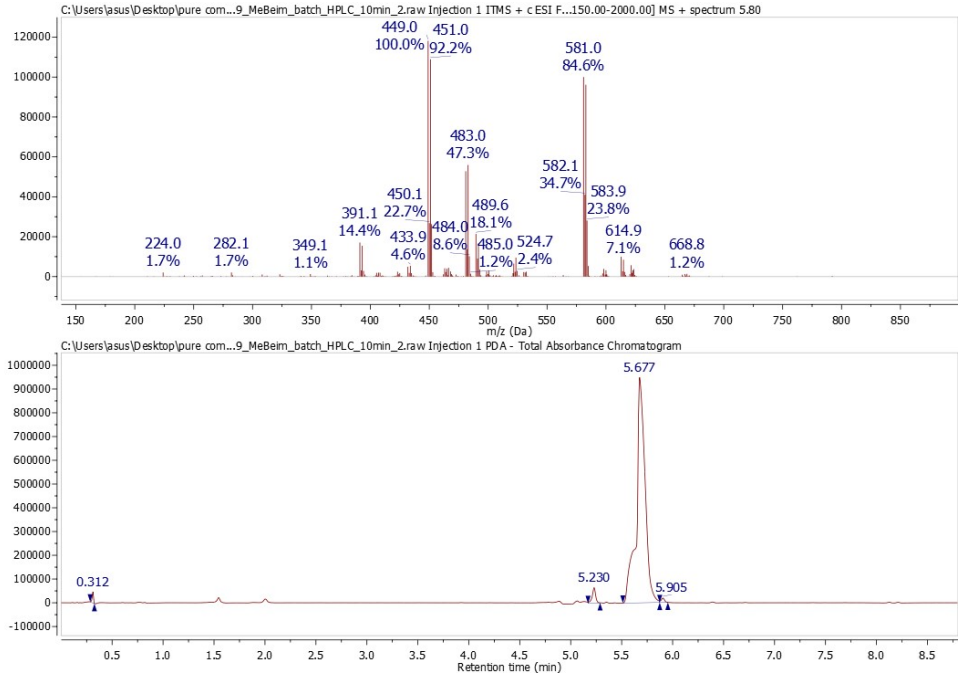

Figure S35. LCMS spectra of MnC9MeBeIm

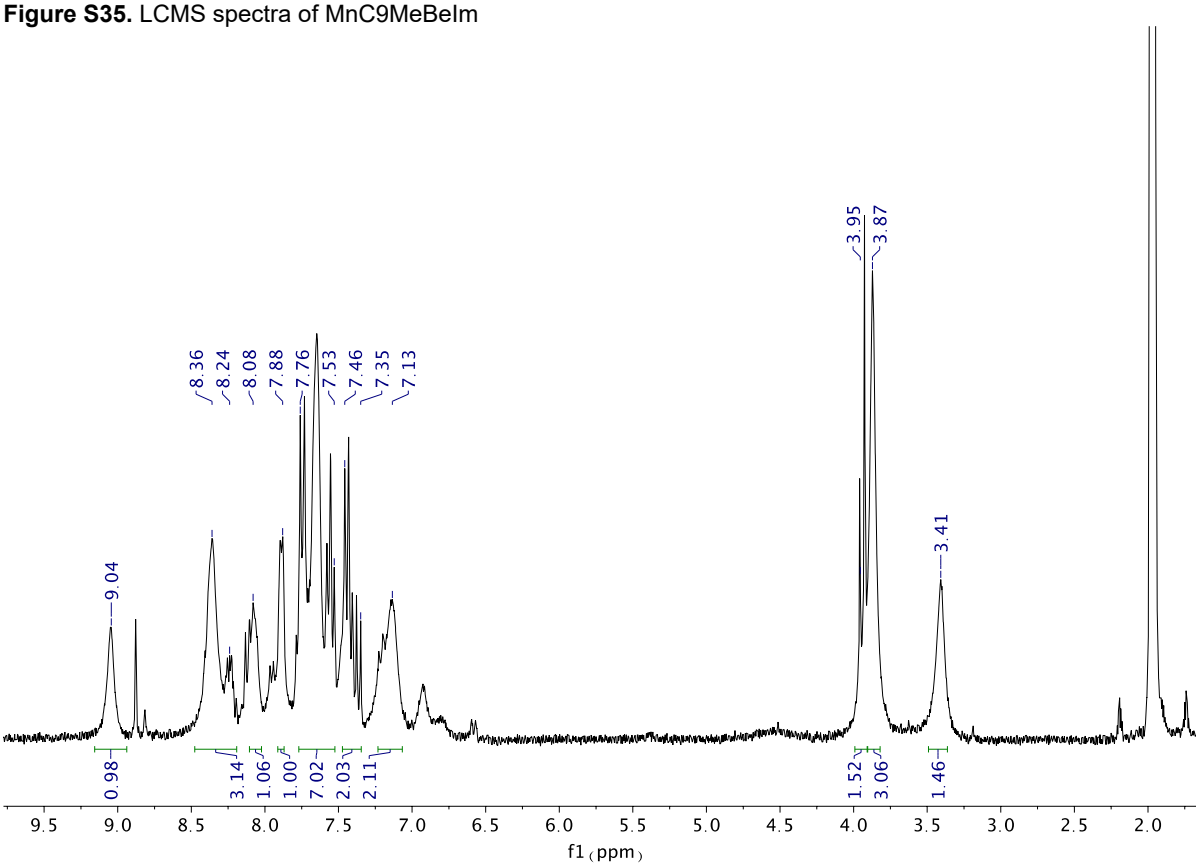

Figure S36. ^{1}H NMR spectra of MnC9MeBeIm (300 MHz, CD3CN) δ 9.04 (1H, s), 8.36-8.24 (3H, br), 8.08 (1H, d), 7.88 (1H, d), 7.76-7.53 (7H, m), 7.46-7.35 (2H, m), 7.13 (2H, br), 3.95-3.87 (4.5H, m), 3.41 (1.5H, s).

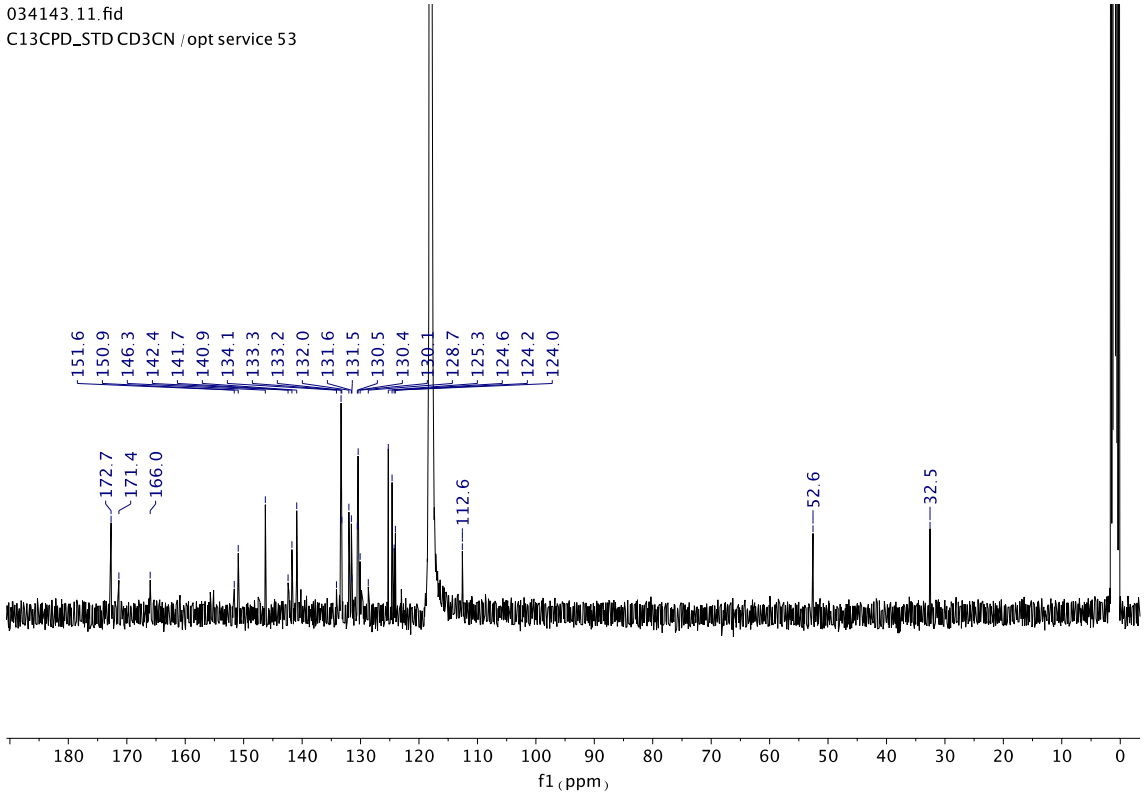

Figure S37. ^{13}C NMR spectra of MnC9MeBeIm (400 MHz, CD3CN) δ 172.7, 171.4, 166.0, 151.6, 150.9, 146.3, 142.4, 141.7, 140.9, 134.1, 133.3, 133.2, 132.0, 131.6, 131.5, 130.5, 130.4, 130.1, 128.7, 125.3, 124.6, 124.2, 124.0, 112.6, 52.6, 32.5.

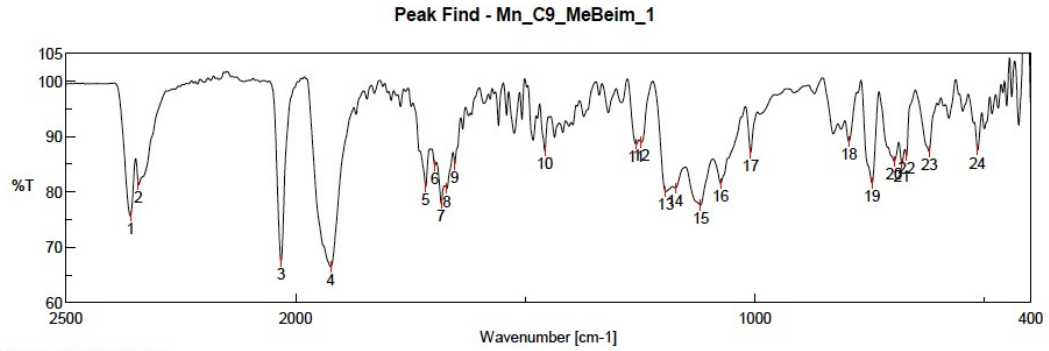

[Result of Peak Picking]

No.	Position	Intensity	No.	Position	Intensity	No.	Position	Intensity
1	2359.48	75.6352	2	2342.12	81.2846	3	2031.64	67.4182
4	1923.65	66.4566	5	1717.3	80.8992	6	1697.05	84.7003
7	1683.55	77.9128	8	1671.02	80.5942	9	1653.66	84.9677
10	1457.92	87.3727	11	1259.29	88.5842	12	1247.72	88.9213
13	1194.69	79.9864	14	1173.47	80.6724	15	1118.51	77.616
16	1075.12	81.5429	17	1009.55	87.0827	18	795.493	89.0454
19	745.352	81.5525	20	697.141	85.4989	21	680.749	85.0268
22	670.142	86.4807	23	620.966	87.2658	24	515.865	87.5248

Figure S38. IR spectra of MnC9MeBeIm (ATR): 2031 cm^{-1}, 1923 cm^{-1} ν CO

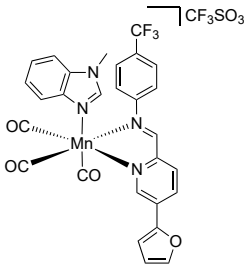

E. Mn**E2**MeBeim

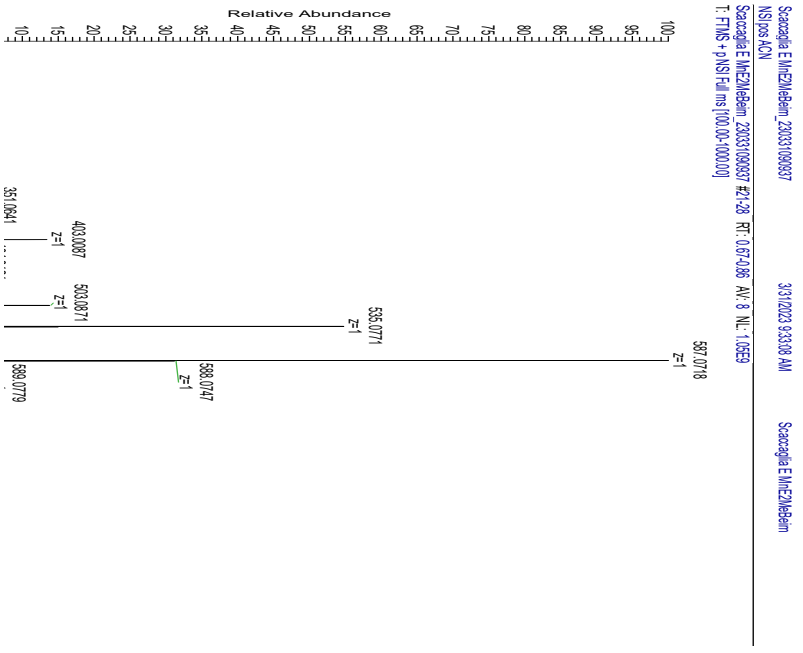

Figure S39. HRMS spectra of MnE2MeBeIm

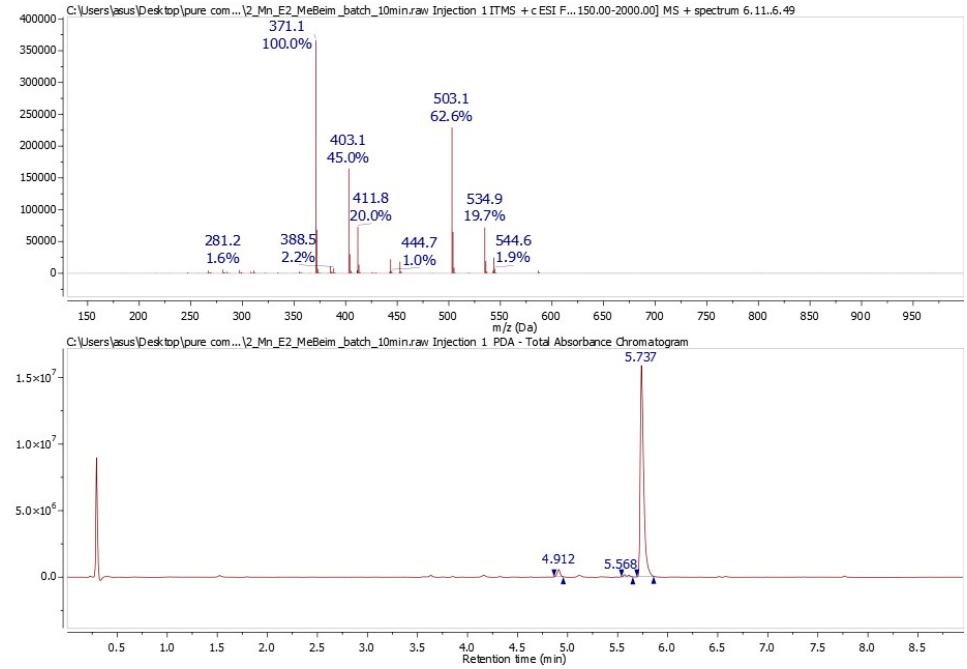

Figure S40. LCMS spectra of MnE2MeBeIm
GA_237147.10.fid

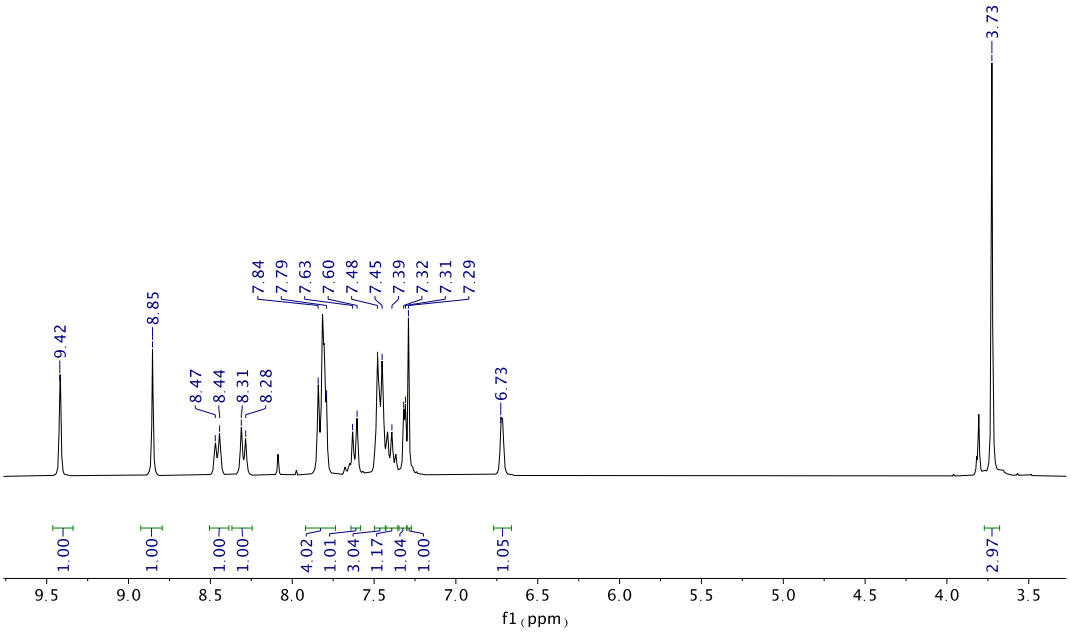

Figure S41. ^{1}H NMR spectra of MnE2MeBeIm (300 MHz, CD3CN) δ 9.42 (1H, s), 8.85 (1H, s), 8.47-8.44 (1H, d), 8.31-8.28 (1H, d), 7.84-7.79 (4H, m), 7.63-7.60 (1H, m), 7.48-7.45 (1H, m), 7.39 (1H, m), 7.32 (1H, d), 7.29 (1H, s), 6.73 (1H, s), 3.73 (3H, s).

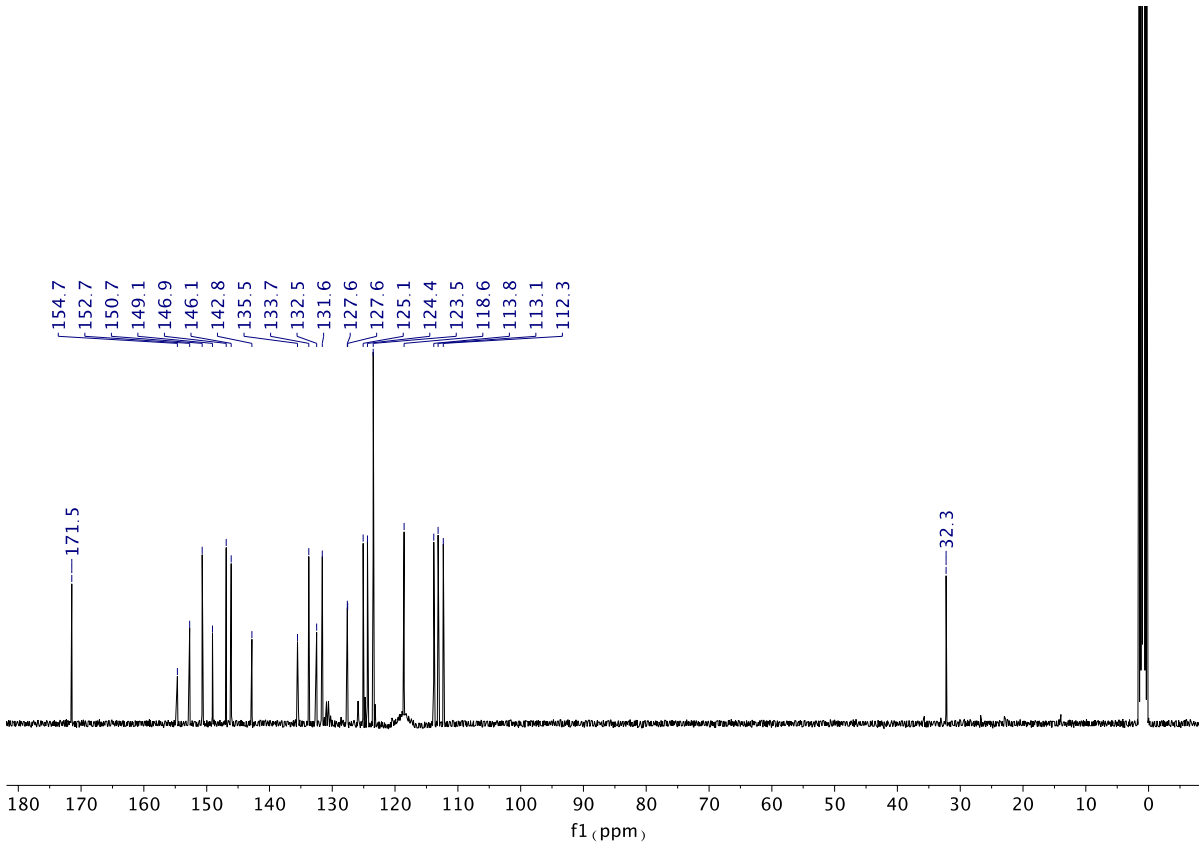

Figure S42. ^{13}C NMR spectra of MnE2MeBeIm (400 MHz, CD_3CN) 171.5, 154.7, 152.7, 150.7, 149.1, 146.9, 146.1, 142.8, 135.5, 133.7, 132.5, 131.6, 127.6, 127.6, 125.1, 124.4, 123.5, 118.6, 113.8, 113.1, 112.3, 32.3.

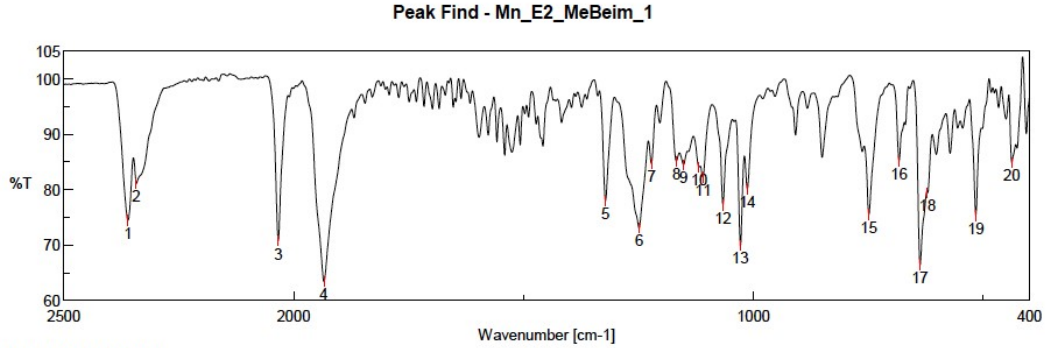

[Result of Peak Picking]

No.	Position	Intensity	No.	Position	Intensity	No.	Position	Intensity
1	2360.44	74.4518	2	2342.12	81.0886	3	2033.57	70.7276
4	1934.25	63.3829	5	1321.96	77.948	6	1248.68	73.0583
7	1221.68	84.6785	8	1167.69	85.0974	9	1152.26	84.4904
10	1118.51	84.0543	11	1109.83	82.2122	12	1066.44	77.2128
13	1028.84	69.9337	14	1013.41	80.091	15	749.209	75.4827
16	683.642	85.1049	17	638.323	66.4329	18	621.931	79.4483
19	516.829	75.3057	20	438.726	84.869			

Figure S43. IR spectra of MnE2MeBeIm (ATR): 2033 cm^{-1}, 1934 cm^{-1} v CO

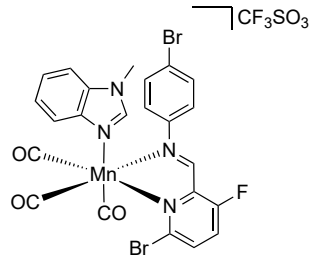

F. Mn**G9**MeBeim

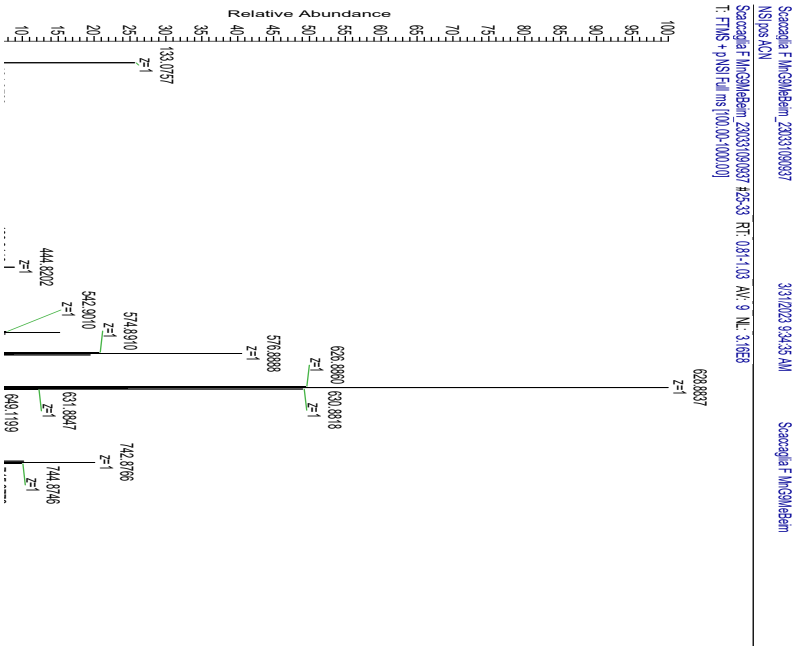

Figure S44. HRMS spectra of MnG9MeBeIm

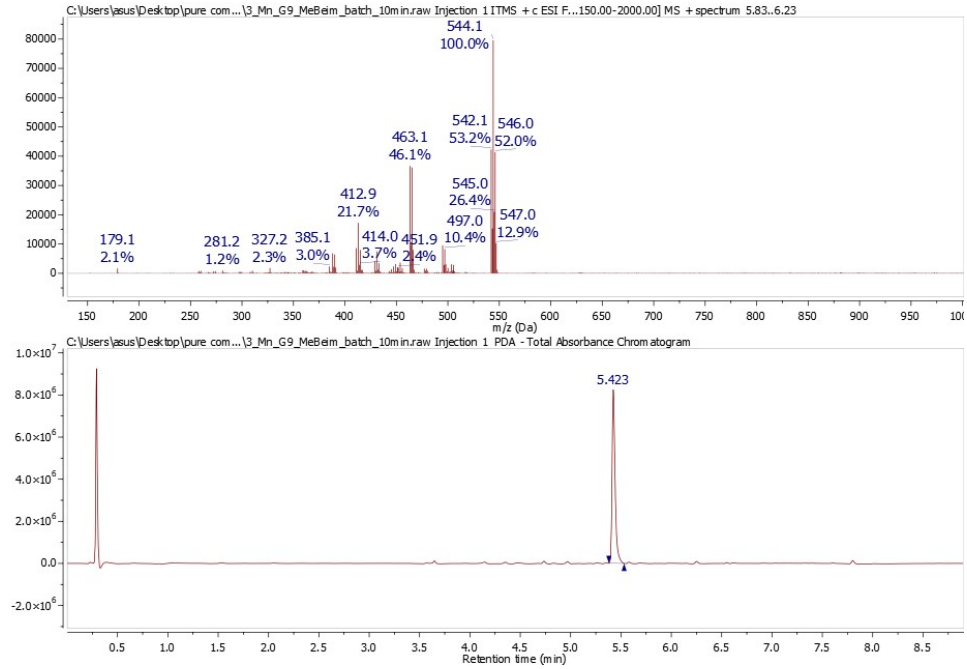

Figure S45. LCMS spectra of MnG9MeBeIm

GA_237098.10.fid

Mn_G9_MeBeim_HPLC

Proton_ns32 CD3CN / opt frei 58

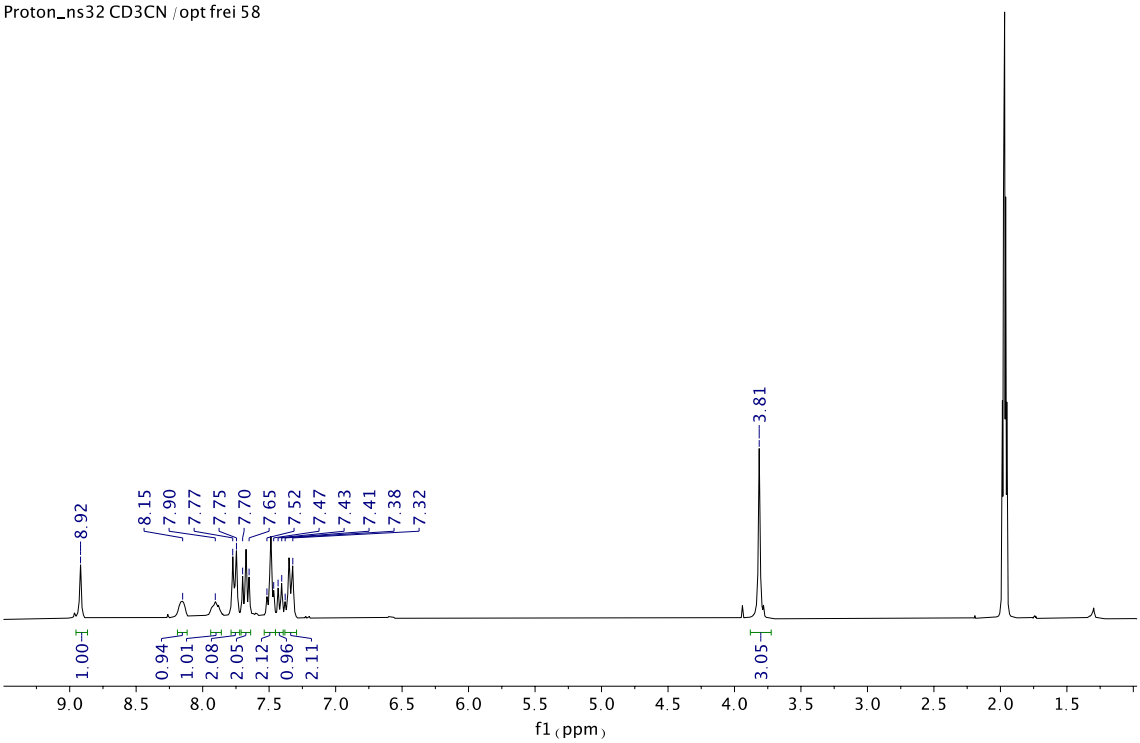

Figure S46. ^{1}H NMR spectra of MnG9MeBeIm (300 MHz, CD3CN) δ 8.92 (1H, s), 8.15 (1H, br), 7.90 (1H, br), 7.77-7.75 (2H, d), 7.70-7.65 (2H, t), 7.52-7.47 (2H, t), 7.43-7.41 (1H, d), 7.38-7.32 (2H, m), 3.81 (3H, s).

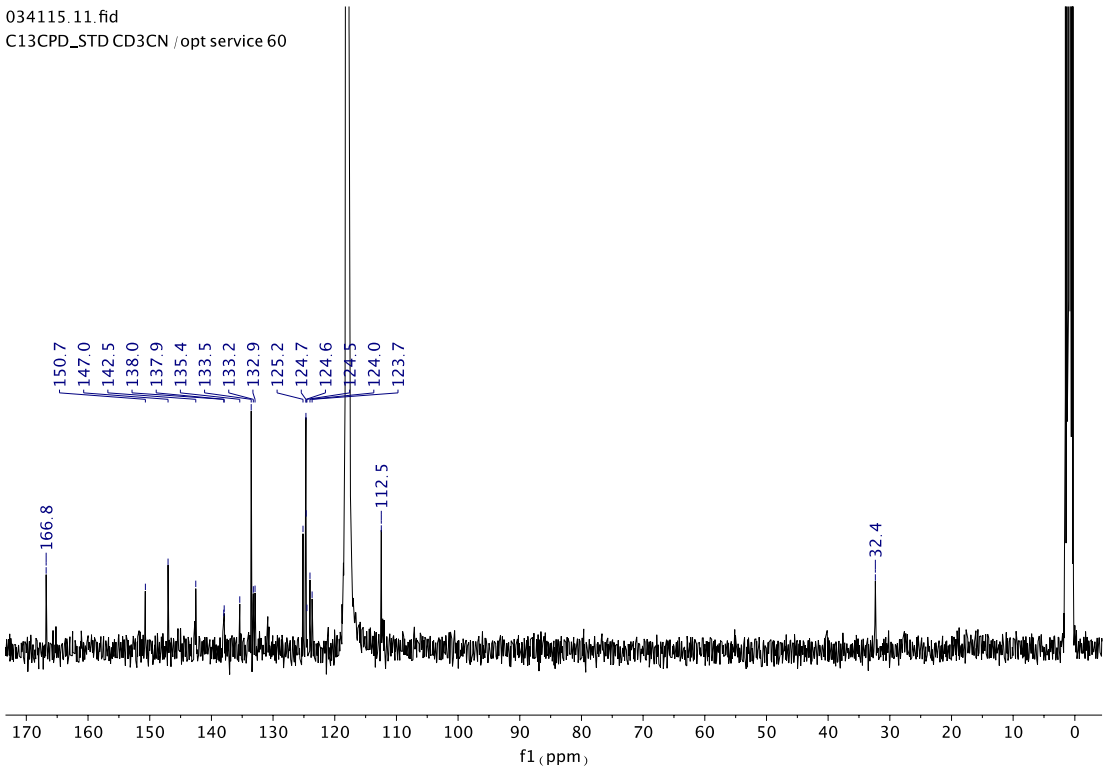

Figure S47. ^{13}C NMR spectra of MnG9MeBeIm (400 MHz, CD_3CN) δ 166.8, 150.7, 147.0, 142.5, 138.0, 137.9, 135.4, 133.5, 133.2, 132.9, 125.2, 124.7, 124.6, 124.5, 124.0, 123.7, 112.5, 32.4.

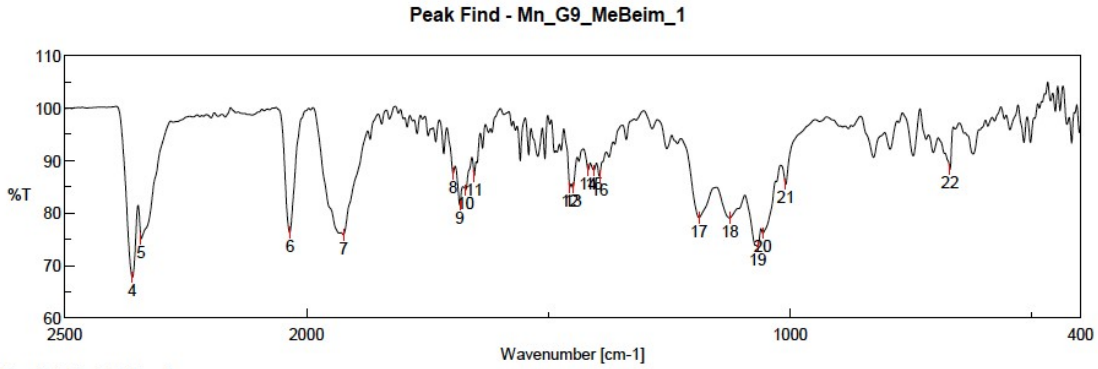

[Result of Peak Picking]

No.	Position	Intensity	No.	Position	Intensity	No.	Position	Intensity
1	2987.2	84.1658	2	2971.77	84.7731	3	2900.41	86.9914
4	2360.44	67.7652	5	2342.12	75.128	6	2034.53	76.2555
7	1923.65	75.8341	8	1697.05	87.4891	9	1683.55	81.481
10	1671.02	84.4165	11	1653.66	87.0137	12	1455.99	84.8505
13	1449.24	84.7941	14	1418.39	88.1605	15	1405.85	88.1037
16	1394.28	86.9979	17	1188.9	79.14	18	1125.26	79.047
19	1067.41	73.5379	20	1056.8	76.1732	21	1009.55	85.4588
22	670.142	88.3291						

Figure S48. IR spectra of MnG9MeBeIm (ATR): 2034 cm^{-1}, 1923 cm^{-1} ν CO

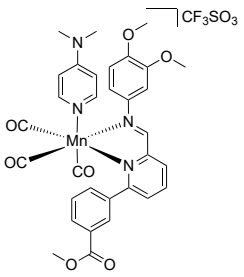

G. Mn**C1**DMAP

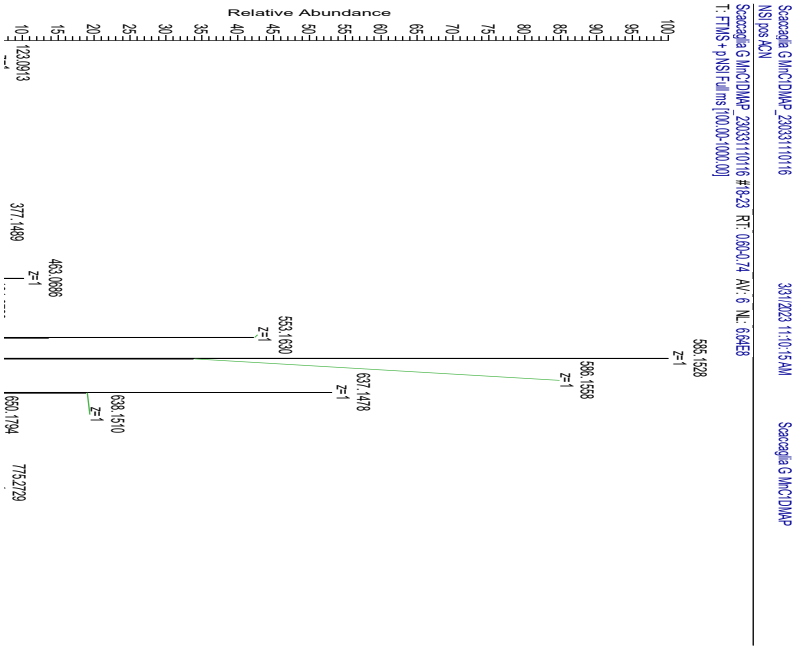

Figure S49. HRMS spectra of MnC1DMAP

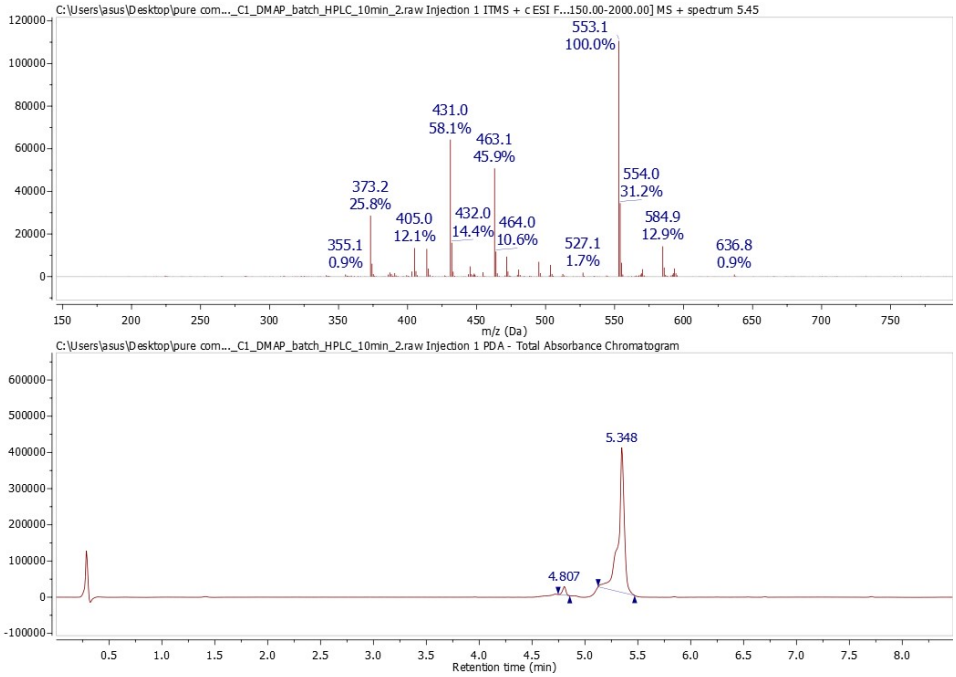

Figure S50. LCMS spectra of MnC1DMAP

GA_239591.10.fid

Mn_C1_DMAP_2ndNMR

Proton_ns32 CD3CN / opt frei 15

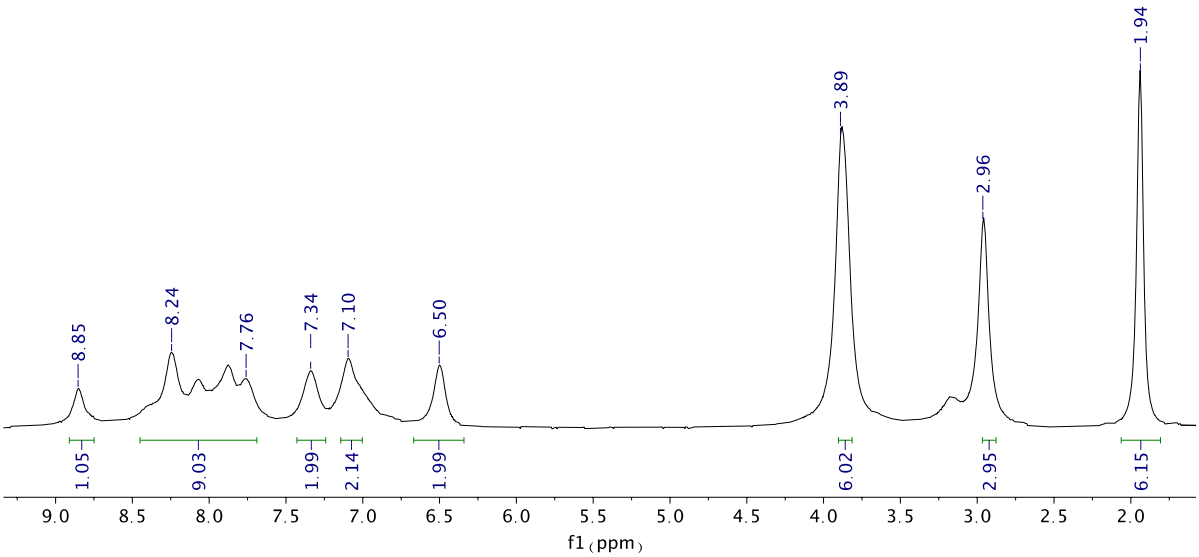

Figure S51. ^{1}H NMR spectra of MnC1DMAP (300 MHz, CD_3CN)) δ 8.85 (1H,br), 8.24-7.76 (9H, m and br), 7.34 (2H. br), 7.10 (2H, br), 6.50 (2H, br), 3.89 (6H, br), 2.96 (3H, br), 1.94 (6H, br).

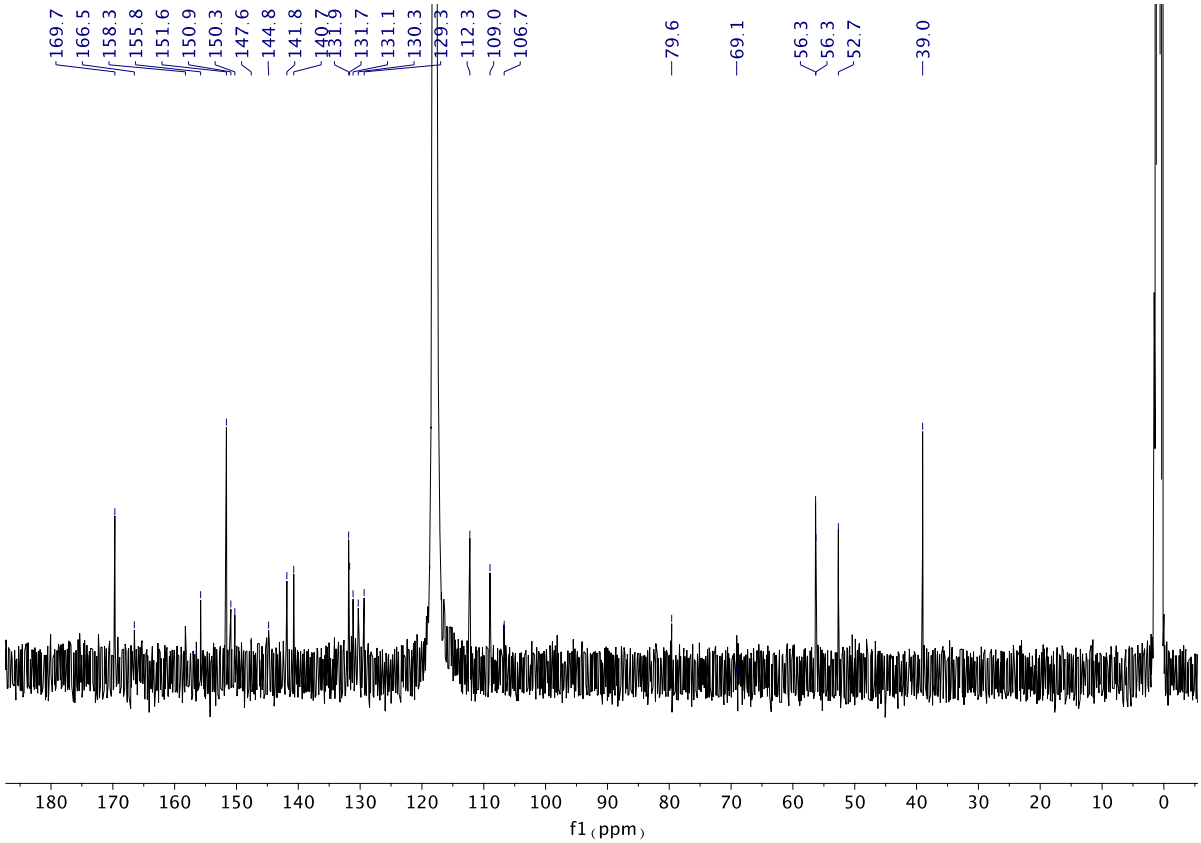

Figure S52. ^{13}C NMR spectra of MnC1DMAP (400 MHz, CD_3CN)) δ 169.7, 166.5, 158.3, 158.2, 156.5, 155.8, 150.9, 150.3, 147.6, 144.8, 141.8, 140.7, 131.9, 131.7, 131.1, 130.3, 129.3, 112.3, 109.0, 106.7, 79.6, 69.1, 56.3, 56.3, 52.7, 39.0.

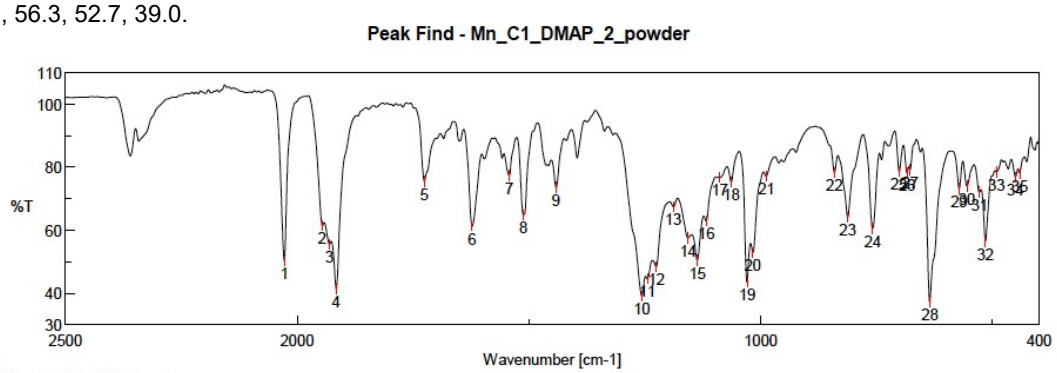

[Result of Peak Picking]

No.	Position	Intensity	No.	Position	Intensity	No.	Position	Intensity
1	2027.78	50.3476	2	1945.82	61.479	3	1930.4	55.4934
4	1915.93	41.412	5	1725.98	75.5271	6	1622.8	61.3586
7	1542.77	77.3962	8	1511.92	64.8316	9	1441.53	73.5613
10	1256.4	39.1944	11	1244.83	44.5929	12	1225.54	48.4228
13	1188.9	67.4362	14	1157.08	57.5832	15	1136.83	50.5095
16	1117.55	62.958	17	1088.62	76.7139	18	1063.55	75.3447
19	1029.8	43.4998	20	1017.27	52.9855	21	988.339	77.1062
22	841.776	78.3476	23	812.849	64.0181	24	758.852	60.5355
25	701.962	78.5798	26	684.606	78.2456	27	677.856	79.2688
28	635.43	37.344	29	572.755	73.2601	30	555.398	74.0295
31	528.4	72.0969	32	515.865	56.5192	33	491.759	78.4908
34	451.261	76.9119	35	441.619	78.1497			

Figure S53. IR spectra of MnC1DMAP (ATR): 2027 cm^{-1}, 1916 cm^{-1} ν CO

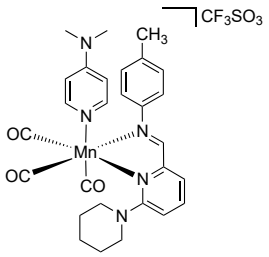

H. Mn**D8**DMAP

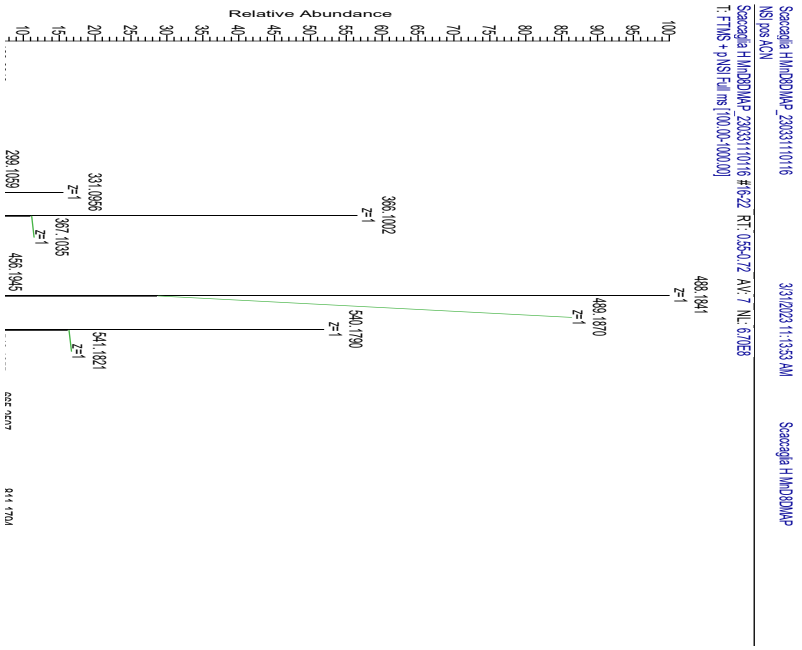

Figure S54. HRMS spectra of MnD8DMAP

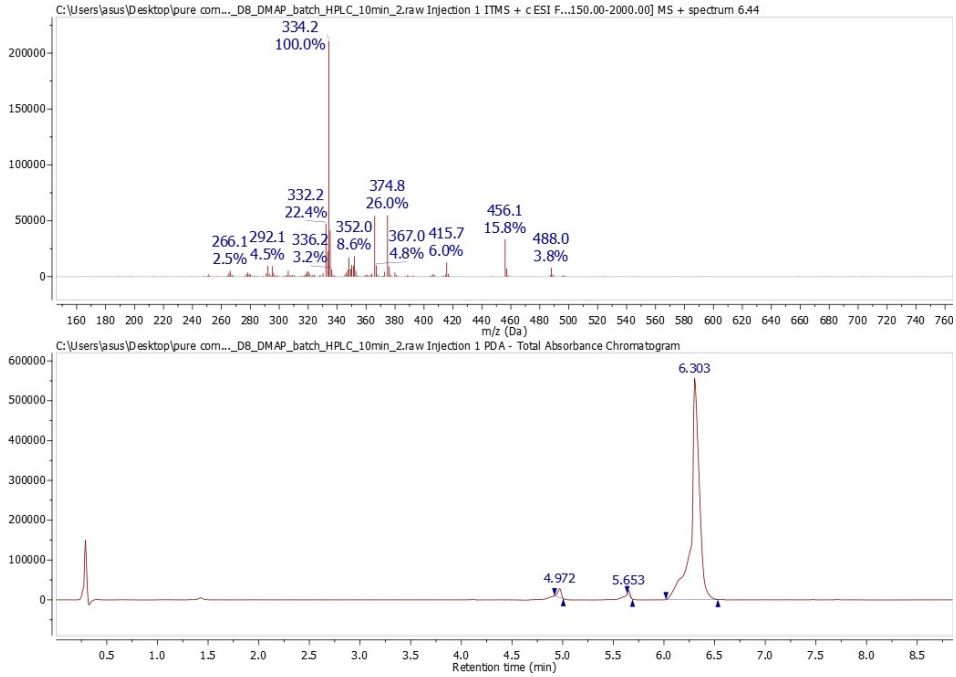

Figure S55. LCMS spectra of MnD8DMAP

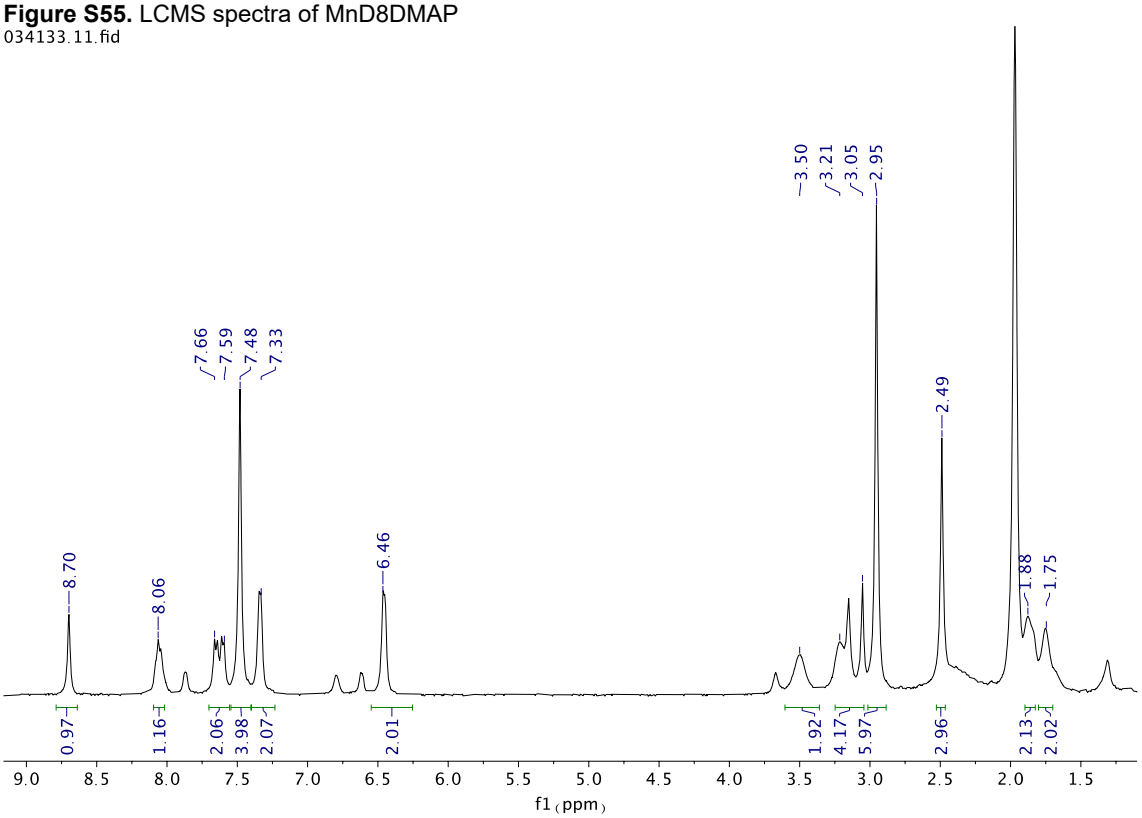

Figure S56. ^{1}H NMR spectra of MnD8DMAP (300 MHz, CD3CN) δ 8.70 (1H, s), 8.06 (1H, m), 7.66-7.59 (2H, m), 7.48 (m, 4H), 7.33 (2H, m), 6.46 (2H, m), 3.50 (2H, br), 3.21-3.05 (4H, br), 2.95 (6H, s), 2.49 (3H, s), 1.88 (2H, br),1.75 (2H, br).

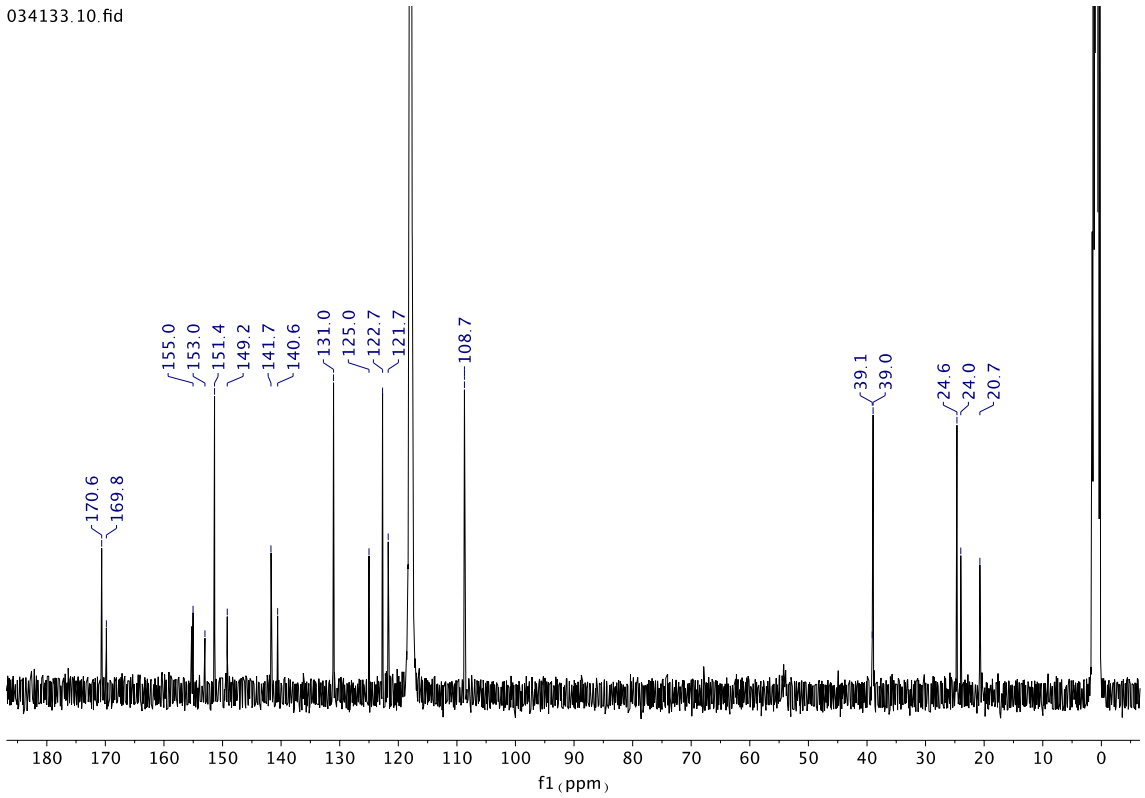

Figure S57. ^{13}C NMR spectra of MnD8DMAP (400 MHz, CD3CN) δ 170.6, 169.8, 155.0, 153.0, 151.4, 149.2, 141.7, 140.6, 131.0, 125.0, 122.7, 121.7, 108.7, 39.1, 39.0, 24.6, 24.0, 20.7.

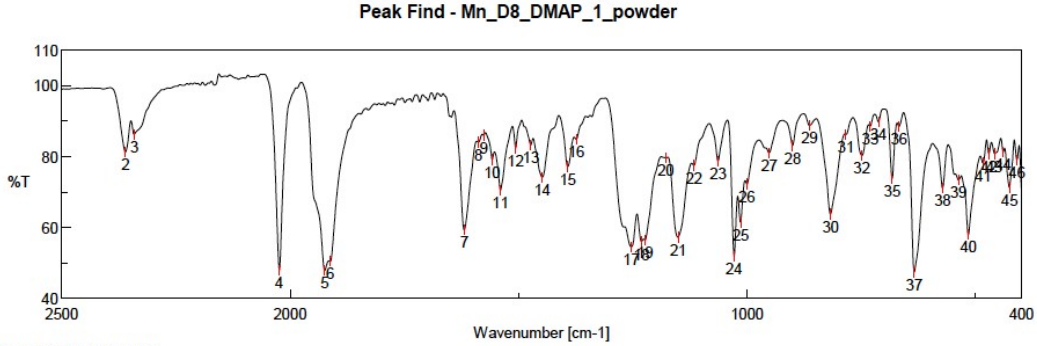

[Result of Peak Picking]

No.	Position	Intensity	No.	Position	Intensity	No.	Position	Intensity
1	2927.41	88.9648	2	2360.44	81.2524	3	2341.16	86.2433
4	2023.93	47.8871	5	1924.61	47.8973	6	1912.07	50.4603
7	1618.95	59.3105	8	1588.09	84.0178	9	1576.52	85.9903
10	1558.2	79.0986	11	1539.88	70.423	12	1507.1	82.3213
13	1473.35	83.2378	14	1448.28	74.1442	15	1392.35	77.1642
16	1374.03	84.8672	17	1253.5	54.5481	18	1231.33	55.9948
19	1223.61	56.4426	20	1178.29	79.5956	21	1151.29	57.2958
22	1116.58	77.5061	23	1063.55	78.714	24	1028.84	51.9694
25	1014.37	61.5006	26	1000.87	72.274	27	951.698	81.0472
28	900.594	83.1239	29	863.953	88.7717	30	817.67	63.757
31	783.922	86.2341	32	749.209	80.2758	33	730.889	88.5416
34	712.569	89.8059	35	682.677	73.7993	36	668.214	88.3944
37	634.466	47.4202	38	572.755	71.0648	39	538.042	73.465
40	515.865	58.0106	41	484.045	78.1571	42	471.51	80.7461
43	458.975	80.8129	44	439.69	81.3501	45	426.191	71.2872
46	409.799	79.0271						

Figure S58. IR spectra of MnD8DMAP (ATR): 2024 cm^{-1}, 1924 cm^{-1} ν CO

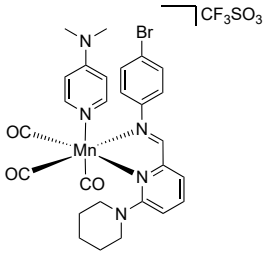

I. Mn**D9**DMAP

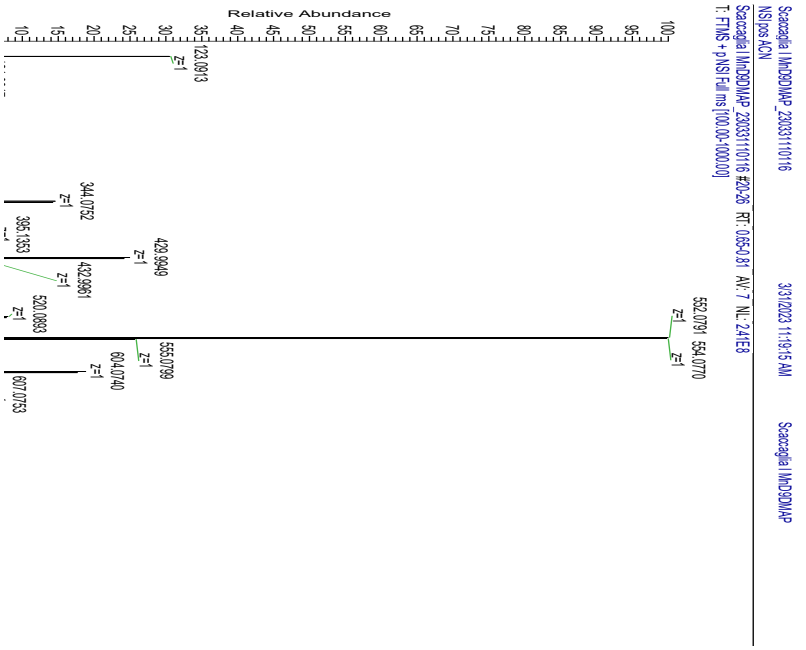

Figure S59. HRMS spectra of MnD9DMAP

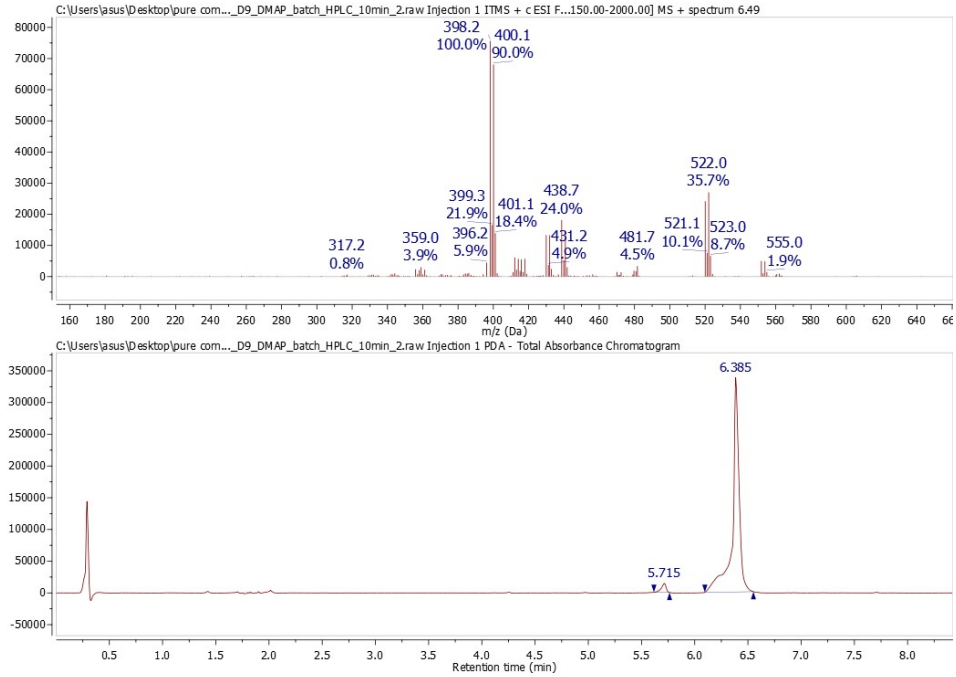

Figure S60. LCMS spectra of MnD9DMAP

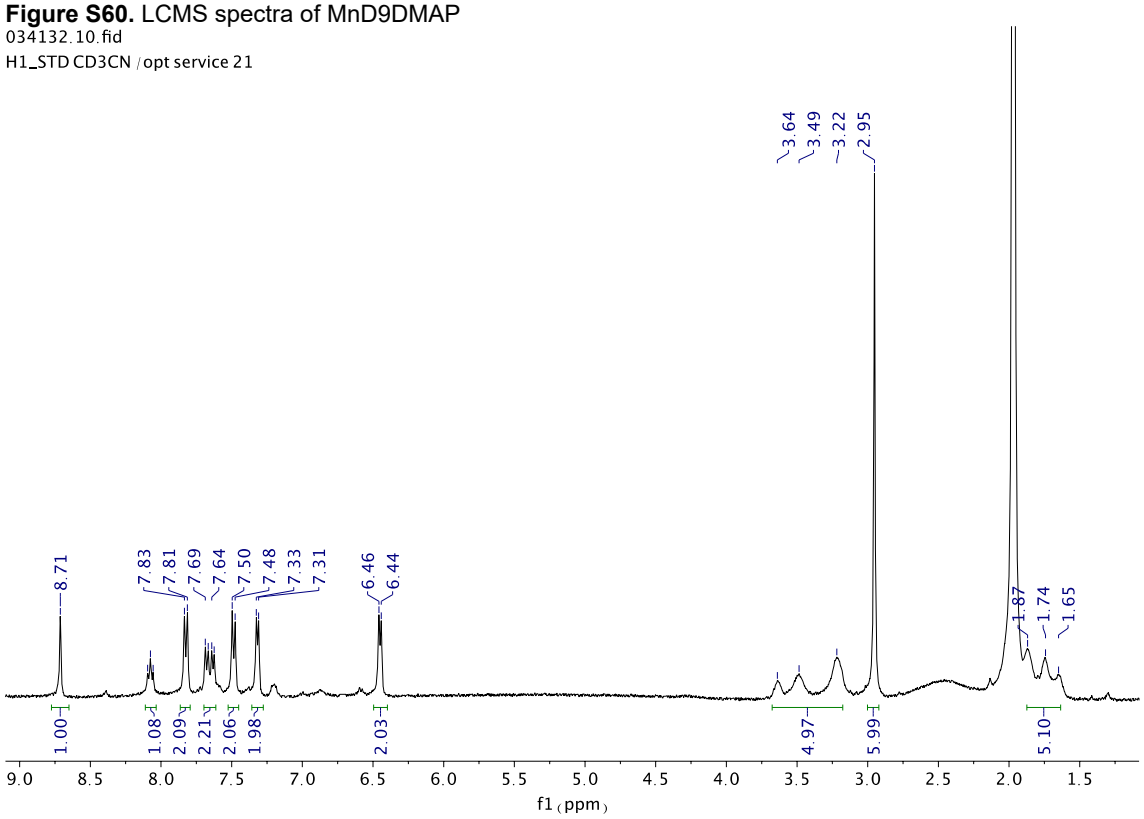

Figure S61. ^{1}H NMR spectra of MnD9DMAP (300 MHz, CD3CN) δ 8.71 (1H, s), 8.08 (1H, t), 7.82 (2H, d), 7.69-7.62 (2H, m), 7.49 (2H, d), 7.32 (2H, d), 6.45 (2H, d), 3.64-3.22 (5H, br), 2.95 (6H, s),1.87-1.65 (5H, br).

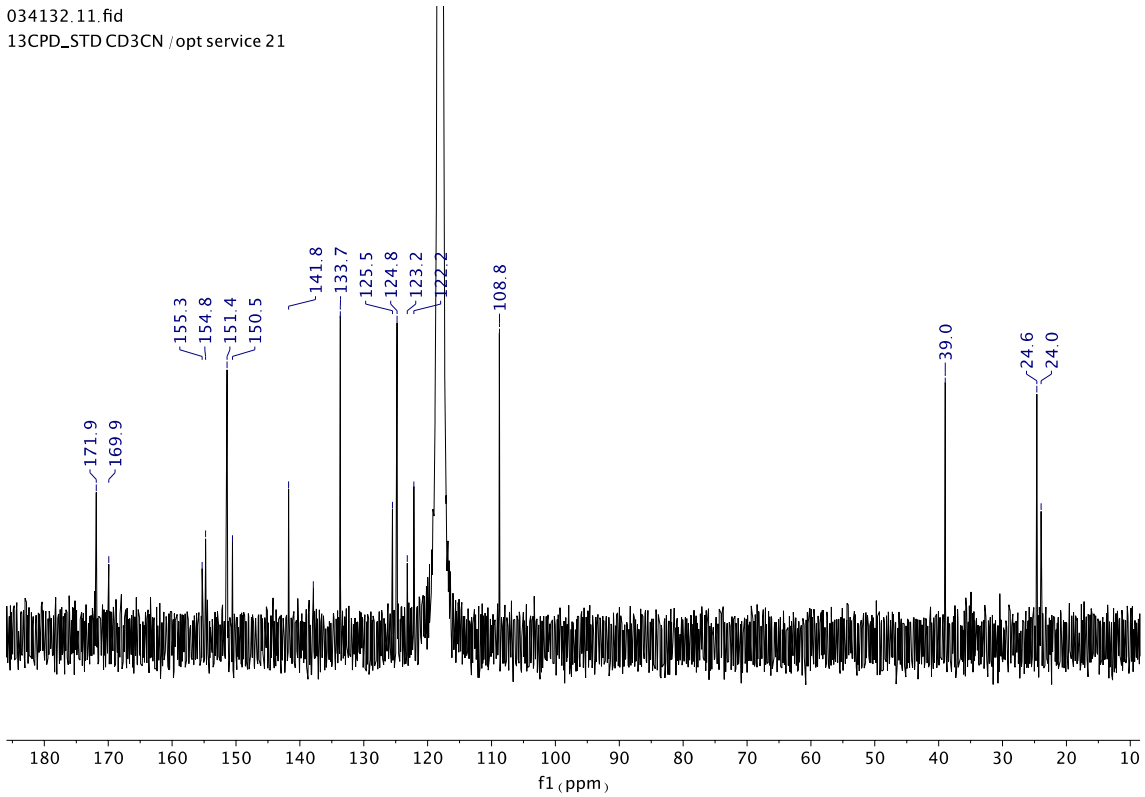

Figure S62. ^{13}C NMR spectra of MnD9DMAP (400 MHz, CD_3CN) δ 171.9, 169.9, 155.3, 154.8, 151.4, 150.5, 141.8, 137.9, 133.7, 125.5, 124.8, 123.2, 122.2, 108.8, 39.0, 24.6, 24.0.

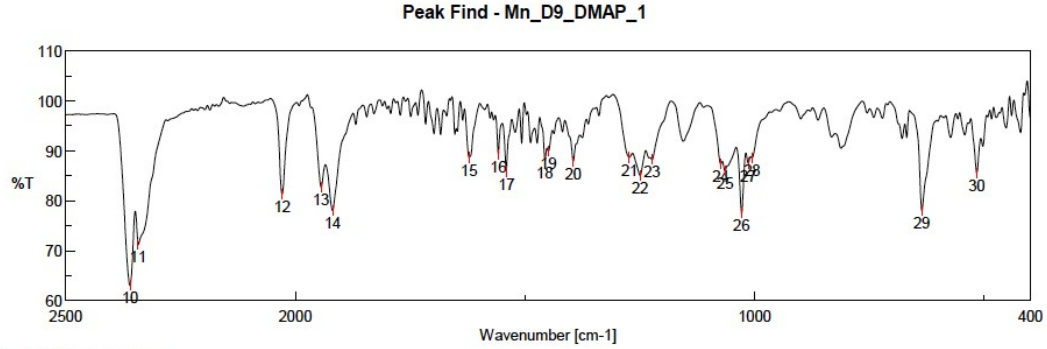

[Result of Peak Picking]

No.	Position	Intensity	No.	Position	Intensity	No.	Position	Intensity
1	3749.9	90.0485	2	3734.48	87.9367	3	3689.16	89.5576
4	3674.69	88.5796	5	3648.66	87.5999	6	2987.2	85.7925
7	2970.8	85.6654	8	2923.56	87.8889	9	2901.38	87.1535
10	2359.48	63.0428	11	2342.12	71.2213	12	2028.75	81.2799
13	1943.89	82.7062	14	1918.82	78.0187	15	1621.84	88.6548
16	1558.2	89.1785	17	1540.85	85.8428	18	1456.96	88.0901
19	1449.24	89.909	20	1395.25	87.8828	21	1272.79	88.6831
22	1249.65	85.0169	23	1223.61	88.2508	24	1074.16	87.3511
25	1064.51	85.9749	26	1028.84	77.5429	27	1014.37	87.5227
28	1005.7	88.5285	29	636.394	77.9952	30	516.829	85.5065

Figure S63. IR spectra of MnD9DMAP (ATR): 2028 cm^{-1}, 1919 cm^{-1} ν CO

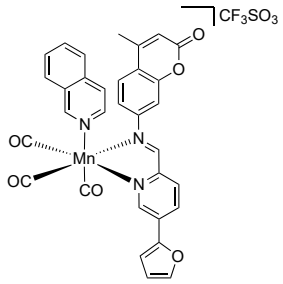

L. Mn**E6**QUIN

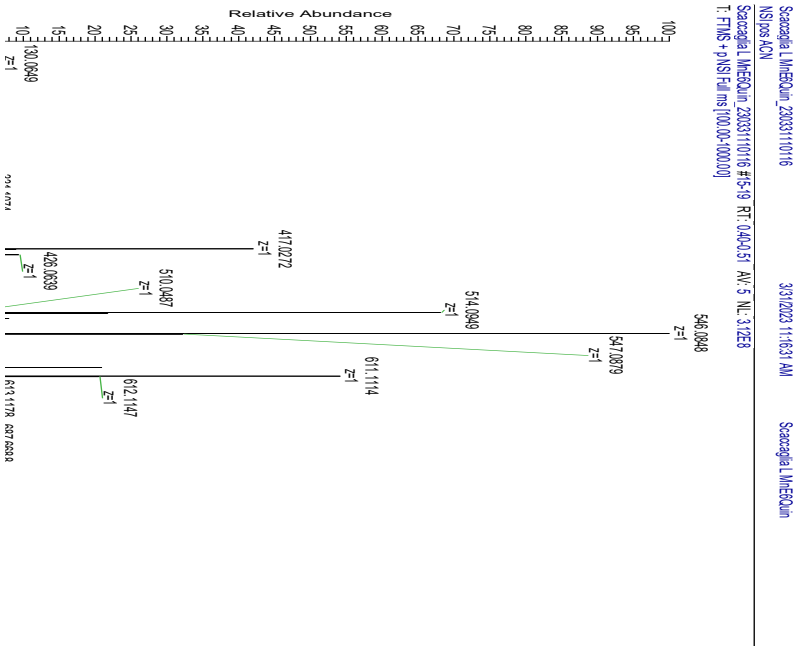

Figure S64. HRMS spectra of MnE6Quin

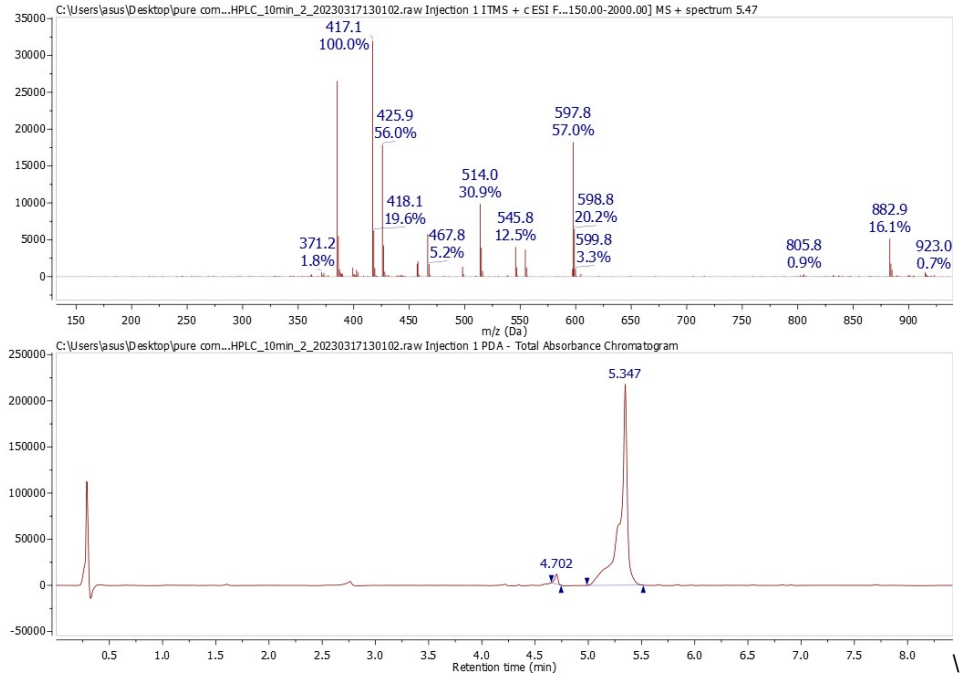

Figure S65. LCMS spectra of MnE6Quin

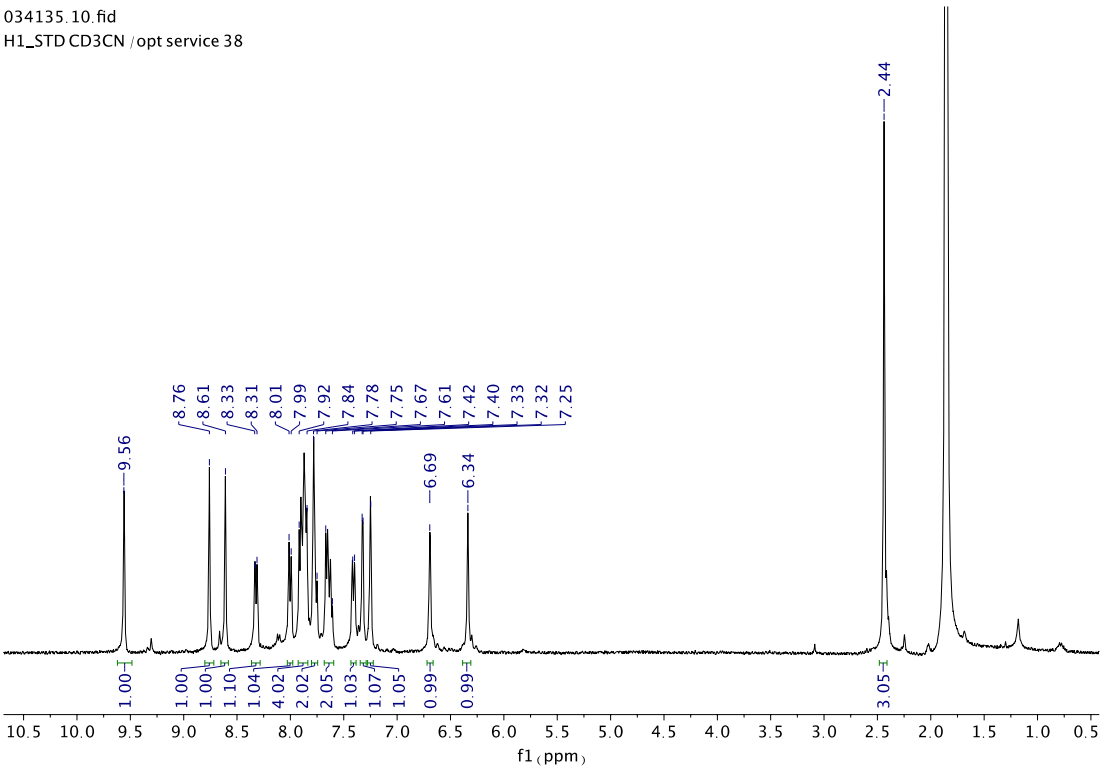

Figure S66. ^{1}H NMR spectra of MnE6Quin (400 MHz, CD3CN) 9.56 (1H, s), 8.76 (1H, s), 8.61 (1H, s), 8.32 (1H, d), 8.00 (1H, d), 7.92 -7.84 (4H, m), 7.78-7.75 (2H, m), 7.67-7.61(2H, m), 7.41 (1H, d), 7.32 (1H, d), 7.25 (1H, s), 6.69 (1H, s), 6.34 (1H), 2.44 (3H, s).

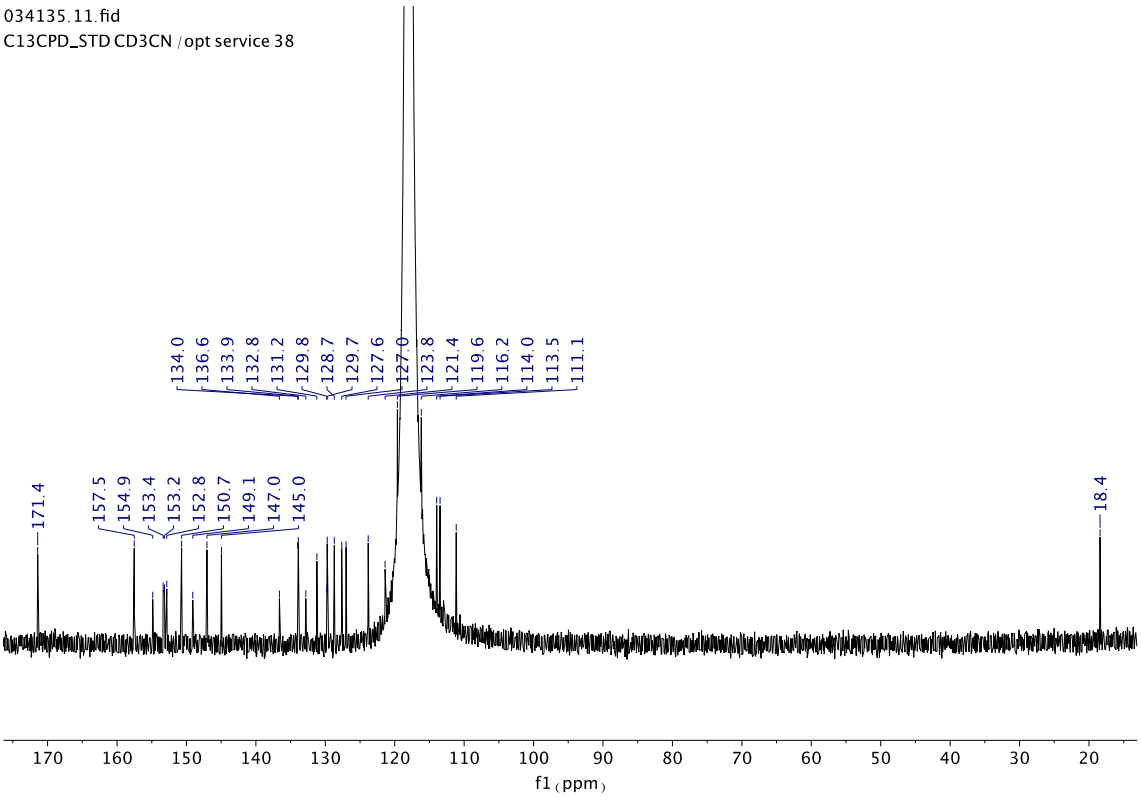

Figure S67. ^{13}C NMR spectra of MnE6Quin (400 MHz, CD3CN) δ 171.4, 157.5, 154.9, 153.4, 153.2, 152.8, 150.7, 149.1, 147.0, 145.0, 136.6, 134.0, 133.9, 132.8, 131.2, 129.8, 129.7, 128.7, 127.6, 127.0, 123.8, 121.4, 119.6, 116.2, 114.0, 113.5, 111.1, 18.4.

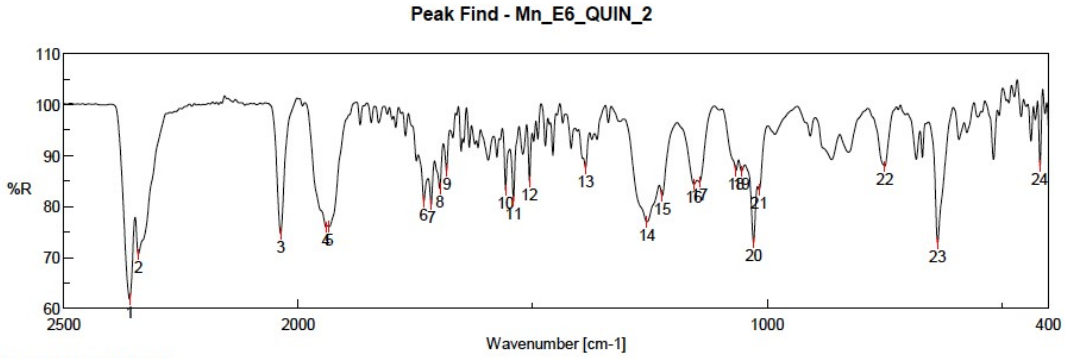

[Result of Peak Picking]

No.	Position	Intensity	No.	Position	Intensity	No.	Position	Intensity
1	2359.48	61.8656	2	2341.16	70.6134	3	2037.43	74.7218
4	1941	75.9592	5	1934.25	76.0686	6	1732.73	80.9271
7	1716.34	80.4095	8	1698.02	83.5836	9	1683.55	87.0362
10	1558.2	83.2552	11	1540.85	81.1146	12	1507.1	84.8845
13	1387.53	87.5184	14	1256.4	76.9779	15	1223.61	82.1176
16	1156.12	84.3485	17	1144.55	84.8039	18	1066.44	87.0257
19	1054.87	86.8905	20	1028.84	72.9291	21	1017.27	83.2927
22	749.209	87.8907	23	636.394	72.8	24	418.477	88.0058

Figure S68. IR spectra of MnE6Quin (ATR): 2037 cm^{-1}, 1941 cm^{-1} ν CO

Analytical Research and Services
Schürch Group

UNIVERSITÄT BERN

Department of Chemistry, Biochemistry
and Pharmaceutical Sciences
Mass Spectrometry Group

Thermal Elemental Analysis

Name: **Angelo Frei**

Summarize Results
Date : 23.11.2023 08:32:34
Method Name : CHN_fluorinated_Compounds
Method Filename : CHN_F 2023_11_22.mth

Sample name	Anal. Date	Inj. Time	(mg)	% Nitrogen	% Carbon	% Hydrogen
MnG9MeBeIm_1	22.11.2023	09:42	1.036	6.42	38.64	1.94
MnG9MeBeIm_2	22.11.2023	09:51	1.082	6.42	38.47	1.87
MnG9MeBeIm_3	22.11.2023	09:59	0.710	6.33	38.71	1.84
3 Sample(s) in Group No : 2						
Component Name	Average	Std. Dev.	% Rel. S. D.		theor.	dev.
Nitrogen	**6.39**	**0.052**	**0.813**		**7.55**	**-1.16**
Carbon	**38.61**	**0.123**	**0.320**		**40.46**	**-1.85**
Hydrogen	**1.88**	**0.051**	**2.725**		**2.04**	**-0.16**

Figure S69. Thermal Elemental Analysis results for MnG9MnMeBeIm**.**

Bibliography

[1] R. Usón, V. Riera, J. Gimeno, M. Laguna, M. P. Gamasa, *J. Chem. Soc. Dalt. Trans.* **1979**, 996–1002.

[2] S. S. Mendes, J. Marques, E. Mesterházy, J. Straetener, M. Arts, T. Pissarro, J. Reginold, A. Berscheid, J. Bornikoel, R. M. Kluj, *ACS Bio Med Chem Au* **2022**.

[3] Bruker, *APEX3, SAINT SADABS. Bruker AXS Inc., Madison, Wisconsin, USA.* **2016**.

[4] G. M. Sheldrick, *Acta Crystallogr. Sect. C Struct. Chem.* **2015**, *71*, 3–8.

[5] G. M. Sheldrick, *Acta Crystallogr. Sect. A Found. Crystallogr.* **2008**, *64*, 112–122.

[6] O. V Dolomanov, L. J. Bourhis, R. J. Gildea, J. A. K. Howard, H. Puschmann, *J. Appl. Crystallogr.* **2009**, *42*, 339–341.

[7] M. N. Burnett, C. K. Johnson, *ORTEP-III: Oak Ridge Thermal Ellipsoid Plot Program for Crystal Structure Illustrations*, Citeseer, **1996**.

[8] C. F. Macrae, I. Sovago, S. J. Cottrell, P. T. A. Galek, P. McCabe, E. Pidcock, M. Platings, G. P. Shields, J. S. Stevens, M. Towler, *J. Appl. Crystallogr.* **2020**, *53*, 226–235.

[9] R. Motterlini, J. E. Clark, R. Foresti, P. Sarathchandra, B. E. Mann, C. J. Green, *Circ. Res.* **2002**, *90*, e17–e24.

[10] W. T. Langeveld, E. J. A. Veldhuizen, S. A. Burt, *Crit. Rev. Microbiol.* **2013**, *40*, 76–94.

[11] R. Y. Huang, L. Pei, Q. Liu, S. Chen, H. Dou, G. Shu, Z. X. Yuan, J. Lin, G. Peng, W. Zhang, H. Fu, *Front. Pharmacol.* **2019**, *10*, 1–12.

[12] E. Zakharova, M. Orsi, A. Capecchi, J. Reymond, *ChemMedChem* **2022**, *17*, e202200291.

[13] M. Wenzel, M. Rautenbach, J. A. Vosloo, T. Siersma, C. H. M. Aisenbrey, E. Zaitseva, W. E. Laubscher, W. Van Rensburg, J. C. Behrends, B. Bechinger, *MBio* **2018**, *9*, e00802-18.

[14] J. D. te Winkel, D. A. Gray, K. H. Seistrup, L. W. Hamoen, H. Strahl, *Front. Cell Dev. Biol.* **2016**, *4*, 29.

[15] M. Wenzel, B. Kohl, D. Münch, N. Raatschen, H. B. Albada, L. Hamoen, N. Metzler-Nolte, H. G. Sahl, J. E. Bandow, *Antimicrob. Agents Chemother.* **2012**, *56*, 5749–5757.

[16] A. Müller, M. Wenzel, H. Strahl, F. Grein, T. N. V Saaki, B. Kohl, T. Siersma, J. E. Bandow, H.-G. Sahl, T. Schneider, L. W. Hamoen, *Proc. Natl. Acad. Sci. USA* **2016**, *113*, E7077–E7086.

[17] D. Saeloh, V. Tipmanee, K. K. Jim, M. P. Dekker, W. Bitter, S. P. Voravuthikunchai, M. Wenzel, L. W. Hamoen, *PLoS Pathog.* **2018**, *14*, e1006876.